Capturing juvenile tree dynamics from count data using Approximate Bayesian Computation

E. R. Lines[1*], M. A. Zavala[2], P Ruiz-Benito[3] and D. A. Coomes[4]

[1]School of Geography, Queen Mary University of London, Mile End Road, London, UK

[2]Forest Ecology and Restoration Group, Universidad de Alcala, Madrid, Spain.

, Madrid, Spain.

[4]Department of Plant Sciences, University of Cambridge, Downing Street, Cambridge, UK

*Corresponding author: e.lines@qmul.ac.uk

**Acknowledgements**

This research was initially funded by a PhD studentship awarded to DAC by Microsoft Research, and later by an STSM grant from the EU PROFOUND COST action awarded to ERL. MAZ and PRB were supported by FUNDIVER (MINECO, Spain; No. CGL2015-69186-C2-2-R). PRB was supported by the TALENTO Fellow Programme (Comunidad de Madrid, 2016-T2/AMB-1665). We gratefully acknowledge the assistance of Drew Purves in using the PPA model. We thank MAPAMA for the access to the Spanish Forest Inventory Data.

**Abstract**

The juvenile life stage is a crucial determinant of forest dynamics and a first indicator of changes to species' ranges under climate change. However, paucity of detailed re-measurement data of seedlings, saplings and small trees means that their demography is not well understood at large scales, and rarely represented in forest models in detail. In this study we quantify the effects of climate and density dependence on recruitment and juvenile growth and mortality rates of thirteen species measured in the Spanish Forest Inventory. Single-census sapling count data is used to constrain demographic parameters of a simple forest juvenile dynamics model based on the Perfect Plasticity Approximation model (PPA) within a likelihood-free parameterisation method, Approximate Bayesian Computation. Our results highlight marked differences between species, and the important role of climate and stand structure, in controlling juvenile dynamics. Recruitment had a hump-shaped relationship with conspecific density, and for most species conspecific competition had a stronger negative effect than heterospecific competition. Mediterranean species showed on average higher mortality and lower growth rates than temperate species, and in low density stands recruitment and mortality rates were positively correlated. Under climate change our model predicted declines in recruitment rates for almost all species. Reliable predictive models of forest dynamics should include realistic representation of critical early life-stage processes and our approach demonstrates that existing coarse count data can be used to parameterise such models. Approximate Bayesian Computation may have wide application in many fields of ecology to unlock information about past processes from single survey observations.

Key-words: Approximate Bayesian Computation; forest inventory; growth; juvenile dynamics; mortality; recruitment; predictive modelling.

## Introduction

Understanding the processes driving juvenile tree dynamics is crucial to making defensible, long-term predictions of forest dynamics and distribution shifts (Kobe et al. 1995, Ibáñez et al. 2007) because filtering at early life stages is a critical determinant of long-term composition (Kobe 1996, Metz et al. 2010, Green et al. 2014). Tree species' distributions have been observed to be shifting under climate change (e.g. Peñuelas et al. 2007), and climate-induced shifts may halve the value of European forests by 2100 (Hanewinkel et al. 2013). The increased availability of large scale, long-term forest inventory datasets has led to dramatic improvements in the understanding of adult tree growth and mortality, but such datasets rarely contain multi-temporal information on individual juveniles. Instead, studies of juveniles have typically involved tracking stems in small plots and/or at only a few sites (e.g. Clark et al. 1998, Ibáñez et al. 2007, Metz et al. 2010, Matías et al. 2011), providing few insights into critical landscape-level dynamics.

Forest dynamics models applied at large scales typically use simplistic approaches to incorporate information about early life stages (e.g. Vanderwel et al. 2013). The most basic approach is to assume that recruitment into the smallest size class is unlimited (Clark et al. 1998); treat recruitment as a function of asymmetric competition for light and shade tolerance (Pacala et al. 1996), a function of stand basal area characteristics (Kolbe et al. 1999), or parameterise recruitment according to ingrowth into a minimum inventory data size class (Vanderwel et al. 2013). In contrast, smaller scale spatially-explicit individual-based models typically use seed dispersal kernels, with seedling establishment in locations with probability dependent on the distance to conspecific adults, species, adult size and shading (e.g. SORTIE, Pacala et al. 1996; TROLL, Jérôme 1999). Parameterisation of this approach requires large amounts of fine-scale multi-temporal data that is often not available at landscape-scales.

Competitive and facilitative processes strongly influence juvenile dynamics, and the presence and density of conspecific and heterospecific adults are well-recognised determinants of seedling establishment and sapling success in reaching the canopy (e.g. Gomez-Aparicio et al. 2008, Comita et al. 2014). These biotic interactions may influence recruitment success and range shifts under climate change (McCarthy-Neumann and Ibáñez 2012, Katz and Ibáñez 2016, Ettinger and HilleRisLambers 2017) but remain under-studied. In addition, seedling recruitment is affected by canopy gaps and competition from understory shrubs (Beckage et al. 2000), soil moisture, drought and precipitation (Urbieta et al. 2008, Gomez-Aparicio et al. 2008, Mendoza et al. 2009), and facilitation through protection from water and radiation stress by 'nurse' plants (Gómez-Aparicio et al. 2004, Gomez-Aparicio et al. 2008, Plieninger et al. 2010).

This study presents a new method to unlock information on recruitment, growth and survival rates of juveniles from large-scale plot networks. Such datasets, though increasingly available to researchers, are not collected with the aim of understanding juvenile dynamics, such as the annual recruitment rates required by many forest dynamics models. In order to use traditional likelihood methods to fit an annual recruitment rate model we would require annual recruitment observations that is typically not available at large scales – so new statistical techniques are needed to extract this information. We use data from two Spanish Forest Inventories (IFN, MMA 1996, 2007) which systematically and periodically re-samples millions of trees with diameter breast height (DBH) > 7.5 cm across the country. Only counts of smaller stems, without tagging or re-measurement, are recorded, so whilst the dynamics of adult trees can be tracked through re-measurement, those of small stems may be viewed a hidden process with no recruitment rate data available to constrain a model to through a likelihood approach. Here, we used a simple forest dynamics simulator based on the Perfect Plasticity Approximation, PPA, model (Purves et al. 2008) to model juvenile dynamics and compare the number of juveniles predicted by the model with actual numbers recorded in the inventory, using the likelihood-free approach, Approximate Bayesian Computation (ABC), to find the best fit juvenile recruitment, growth and mortality model parameters. ABC is unlike other model fitting methods because it does not require the computation of a likelihood function calculated from response data (data on individual juvenile stem recruitment or dynamics) for models, and can parameterise a model using summary data only (such as our stem count data). ABC has huge promise as a method in systems where the data needed to accurately describe processes is unavailable or not practical to collect (Beaumont, 2010). ABC is increasingly used in areas including epidemiology and genetics (Bertorelle et al. 2010) and, to a lesser extent, ecology (Jabot and Chave 2009, Csilléry et al. 2010, Clarke et al. 2016).

The Mediterranean is a biodiversity hotspot highly vulnerable to the effects of climate change (Thuiller et al. 2005) and defensible projections of species' distribution changes is a pressing need. Climate change may be accelerating low regeneration in some Spanish forests, and concerning mismatches between juvenile and adult distributions have been observed (e.g. Plieninger et al., 2010; Urbieta et al., 2011). Our results quantify the variation in recruitment and juvenile growth and mortality between species and functional groups, trade-offs in rates at the juvenile life stage, test the influence of climate and con- and hetero-specific competition on juvenile performance, and predict changing rates under climate change.

## Materials and methods

### *The Approximate Bayesian Computation (ABC) approach*

ABC methods represent a significant statistical advance in fitting models when the likelihood cannot be formulated or is computationally prohibitive to analyse (Sisson et al. 2007). ABC estimates model parameters for complex processes where only coarse-scale, aggregated data are available (as here, where annual recruitment rates are not known but total numbers of small stems are observed). To fit the particle (parameter set) $p$ of a given model $f$ (the forest simulation model in our application), which predicts an quantity $y$. Without observed data of $y$, $y_0$, we cannot use a likelihood approach to estimate the posterior of $p$. However, with data on one or more observed summary statistics of $y$, $S(y_0)$, we can use ABC to infer best-fit values *p* using a rejection algorithm, thereby approximating the posterior.

Here, we used an ABC Sequential Monte Carlo algorithm (ABC-SMC; Sisson et al. 2007, Beaumont et al. 2009). ABC-SMC repeatedly resamples from previous sets of particles with decreasing tolerance levels, producing a series of sets of particles representing improving approximations to the true posterior. ABC-SMC works as follows: for iterations $t$=1...$T$, $N$ independent particles are sampled from the distribution $\pi(p|d(S(y_0), S(\hat{y})) \leq \varepsilon_t)$, with $\varepsilon_1 > \varepsilon_2 > ... > \varepsilon_T \geq 0$. If t>1, particles are sampled from the previous distribution (*t-1*), using weighted sampling (weights $\omega_i^{(t-1)}$) particles that better approximate $\pi(p|y)$ are re-sampled more often:

**ABC-SMC**

**1.** When t=1, for i=1...*N*

**a.** Sample particles from the prior, $p_i^{(1)} \sim \pi(p)$, and generate $\hat{y} \sim f(y|p_i^{(1)})$ until $d\big(S(y_0), S(\hat{y})\big) < \varepsilon_1$,

**b.** Set all weights equal, as $\omega_i^{(1)}$= *1/N*,

**c.** Set $\Sigma_1$ to be twice the empirical variance of particles $\left\{p_j^{(1)}\right\}$.

**2.** For *t*=2...*T*

**a.** For *i*=1...*N*

**i.** Sample particle *p** from the previous particle distribution, denoted $\left\{p_j^{(t-1)}\right\}$, with weights $\omega_j^{(t-1)}$,

**ii.** Perturb *p** according to a transition kernel, $p^{**} \sim N(p^*|\Sigma_{t-1})$,

**iii.** Use the simulation model $f$ to generate $y^{**} \sim f(y|p^{**})$. If $d\big(S(y_0), S(y^{**})\big) < \varepsilon_t$, set $p_i^{(t)} = p^{**}$, otherwise return to **2ai**.

**b.** For *i*=1...*N*

Calculate the weight of each particle according to:

$$\omega_i^{(t)} \propto \frac{\pi\left(p_i^{(t)}\right)}{\sum_{j=1}^{N} \omega_j^{(t-1)} K_t\left(p_i^{(t)}|p_j^{(t-1)}\right)}$$

where $K_t\left(p_i^{(t)}|p_j^{(t-1)}\right)$ is the multivariate normal density with variance $\Sigma_{t-1}$.

**c.** Set $\Sigma_t$ to be twice the empirical variance of particles $\left\{p_j^{(t)}\right\}$. **(1)**

The ABC-SMC algorithm described in eqn 1 fit our model's parameters, but suffered low acceptance rates (frequent rejection at 2aiii), and was slow to deliver the full particle sample. We therefore used a modified ABC-SMC with adaptive weighting, ABC-SMC-AW (Bonassi and West 2015). ABC-SMC-AW alters the weighting $\omega_j$ of each particle $p_j$ according to the value of the metric $d\left(S(y_0), S\big(f(y|p_j)\big)\right)$, drawing particles with new weights $\nu_j$ at step 2ai in eqn 1, calculated as follows:

$$\text{for } j=1...N \qquad \hat{v}_j^{(t-1)} \propto \omega_j^{(t-1)} K_t\left(S(y_0)|S\left(f\left(y|p_j^{(t-1)}\right)\right)\right)$$

$$\text{for } j=1...N \qquad v_j^{(t-1)} = \frac{\hat{v}_j^{(t-1)}}{\sum_{i=1}^{N} \hat{v}_i^{(t-1)}} \qquad \textbf{(2)}$$

Here, $K_t$ is a multivariate normal distribution with variance equal to the empirical variance of $S\left(f\left(y|p_j^{(t-1)}\right)\right)$.

*Forest Inventory Data*

Data came from the second and third Spanish Forest inventories (IFN2 and IFN3; MMA, 1996, 2007), which sampled over 70,000 re-measured plots systematically on a 1 km$^2$ grid across Spain. IFN plots were sampled using a variable radius concentric plots. All trees DBH > 7.5 cm were measured in a plot of radius 5 m, DBH > 12.5 cm in a plot radius 10 m, DBH > 22.5 cm in a plot radius 15 m and DBH > 42.5 cm in a plot radius 25 m. In the central 5 m radius plot, counts of ‘large saplings’ with heights > 130 cm and DBH in the range 2.5 - 7.5 cm were recorded, along with a categorical measure of the presence/absence of ‘small saplings’ (heights > 130 cm and DBH < 2.5 cm). Here we refer to all stems between 1 cm and 7.5 cm DBH as ‘juveniles’.

We used plots with no recorded management or unnatural source of regeneration recorded in the IFN3, and without planted pines stems, following Ruiz- Benito et al. (2012). We selected 13 species to parameterise models of juvenile dynamics for; all had at least 300 plots containing at least one adult tree (Fig. 1). These comprised seven conifers and six angiosperms; temperate conifers (*Pinus sylvestris, Pinus uncinata)*, Mediterranean confiers (*Pinus pinea, Pinus halepensis, Pinus nigra, Pinus pinaster, Juniperus thurifera*), temperate angiosperms (*Quercus petraea, Quercus pyrenaica, Fagus sylvatica*) and Mediterranean angiosperms (*Quercus faginea*, *Quercus ilex*, *Quercus suber*,). Small stems may be either saplings or resprouts (a common feature of some Mediterranean oaks; Grove and Rackham, 2001), but we were unable to differentiate between these in the data.

*Overview of the modelling approach*

The number of juvenile stems occurring in an inventory-plot is the result of both establishment and demographic processes. We characterised four key processes - the probability of occurrence of juveniles in a plot, the annual rate of recruitment of new stems, and the growth and mortality rates of juveniles. We used a multi-step Bayesian model-fitting approach describe below to parameterise these from the inventory data, separating climate and forest structural effects on recruitment. The first and second processes relate to recruitment: we chose to determine the *probability* of juvenile occurrence by climate, and the annual recruitment *rate* using conspecific density and competitive factors. Fitting these two separately (following Zhu et al. 2015) avoided overfitting and allowed us to make best use of the data available by incorporating all inventory information on stems < 7.5 cm DBH. The probability of juvenile occurrence was estimated using an MCMC approach on inventory presence/absence data, and recruitment, growth and mortality rates were estimated using the ABC approach with a forest simulator (the PPA) and inventory juvenile count data.

*MCMC-derived estimates of probability of occurrence of juveniles*

First, we quantified the probability of the occurrence of juveniles of any size of each species as a function of climatic conditions. We extracted annual precipitation (AP, mm), mean annual temperature (AVT, °C) and drought length (DL, months) from Gonzalo Jiménez (2010). We used inventory information on large and small saplings to calculate presence/absence information for 58,616 unmanaged plots in IFN3. We used MCMC to fit the probability of the occurrence of juveniles, tested logistic models with climatic predictors in quadratic form in all possible permutations, and compared models using AIC (see supporting information, Tables S8 – S10). The best-fit model was:

$$P(occurence) = \frac{1}{1+\exp(-k)}, \text{ where}$$

$$k = a_0 + a_1 a_2 AVT - a_2 AVT^2 + a_3 a_4 AP - a_4 AP^2 + a_5 a_6 DL - a_6 DL^2 \quad \textbf{(3)}$$

We assigned positive priors for parameters $a_1 - a_6$ , resulting in prior quadratic maxima within the climatic ranges of the data.

*Annual juvenile recruitment rate*

We hypothesis that recruitment rates increase with conspecific adult density (potential parent trees), and are impacted by con- and hetero-specific competition. We used crown area index (CAI, projected crown area per unit of ground) to represent both. CAI has been used within several forest models (e.g. Bohlman and Pacala 2011, Coomes et al. 2012, Vanderwel et al. 2013) and was a good predictor for our data in growth and mortality functions (see below, and supporting information Tables S1 – S7). We applied species-specific crown width allometric equations to calculate CAI of all adults (>7.5 cm DBH) ($CAI_{all}$) and of conspecifics only ($CAI_{sp}$) in each inventory plot (allowing for the variable-radius plot structure), for both inventories to calculate temporal changes in competitive environment within the simulations (see supporting information text and Tables S1-S3, Fig. S1).

We define and model recruitment rate as:

$$\text{\# new stems growing through a 1 cm DBH threshold per year} = p_0 CAI_{sp} \exp(-p_1(CAI_{all} - CAI_{sp}) - p_2 CAI_{sp}) \quad \textbf{(4)}$$

Where $p_0 - p_2$ are parameters fit by the ABC-SMC-AW algorithm. We define the *expected annual rate of recruitment* of a species in a given 5 m radius subplot as the probability of recruitment occurring (eqn 3) multiplied by the rate of recruitment (eqn 4).

*Juvenile growth and mortality rates constrained by informative priors*

Many different recruitment, growth and mortality rates could combine to give the observed stem counts, yet not all are reasonable given ecological knowledge of demographic processes. We constructed priors for growth and mortality rates of juveniles small adult tree data in the inventories. We fitted species-specific growth and mortality functions to data from re-measured trees 7.5 - 10 cm DBH within an MCMC framework, comparing alternative models containing size and competition effects using AIC. The best-fit models were:

$$\text{Annual growth rate (cm/year)} = p_3 DBH/(\,1 + p_4 CAI_{all}) \quad \textbf{(5)}$$

$$\text{Annual mortality rate} = logit(k)\ ;\ k = p_5 + p_6 DBH + p_7 CAI_{all} \quad \textbf{(6)}$$

(see supporting information text and Tables S4 – S8, Figs S2 and S3 for a full methodology and results). These functional forms were used within the simulation model (eqn 7 below), with juvenile growth and mortality parameter values $p_3 - p_7$ fit within the ABC-SMC-AW framework. Parameter values from the small adult data were used as strong priors for parameters $p_3 - p_7$ within the ABC-SMC-AW framework.

*Simulation model*

We used a simple cohort-based forest dynamics model to generate juvenile tree densities that were compared with the inventory count data using the ABC-SMC-AW framework (eqns 2, 3). The model simulated size structure and density of juveniles in each plot from their recruitment, growth and mortality rates, taking plot data on climate and competitive environment as inputs. Our simulator was based on the PPA model of Purves et al. (2008) which simulates cohorts rather than tracking individual stems, reducing complexity whilst retaining the ability to reproduce many of the features of spatially explicit models (Strigul et al. 2008). We simulated dynamics over 100 years (time steps) using annual time steps to reduce census interval-dependence of results (Kohyama et al. 2018), with species fitted separately. For each cohort *i* at time *t* we recorded the density $den_{i,t}$ (#stems / 5 m radius plot) and diameter $DBH_{i,t}$ (cm). After 100 time steps densities for all cohorts in the range 2.5 cm < DBH < 7.5 cm were summed to give a model-predicted density directly comparable to the inventory count data. The simulation model ran independently on each plot, as follows:

**Forest dynamics simulation model (based on PPA):**

For each time step (*t*=1...T)

**1.** Calculate plot conditions ($CAI_{all}$ and $CAI_{sp}$) for time *t*.

**2.** For all existing juvenile cohorts (*i*=1...N)

a. Reduce stem density according to the mortality rate (eqn 6):

$den_{i,t}$=(1-P(mortality$_{i,t-1}$)) x $den_{i,t-1}$

b. Increase stem size according to the growth rate (eqn 5):

$DBH_{i,t}$ = $DBH_{i,t-1}$ + growth

**3.** With probability according to climatic conditions (eqn 3), create a new cohort of stems with DBH = 1 cm, with density according to the recruitment rate (eqn 4).

**(7)**

*Implementation of ABC-SMC-AW to derive juvenile demographic rates*

We set wide uniform positive prior distributions for recruitment parameters (eqn 4): $p_0$~U[0,50], $p_1$~U[0,5] and $p_2$~U[0,5]. Note that the ABC-SMC-AW algorithm could select negative values for $p_1$ and $p_2$ –for example to represent a facilitation– if data support was strong. For parameters $p_3$-$p_7$ (eqns 6 and 7) we used Gaussian priors with means set to the means fitted on small adult growth and mortality data (supporting information Tables S6 and S7) and standard deviations set as 10% of the MCMC posterior estimate. Prior distributions were used as initial sampling distributions for all parameters.

We chose two summary statistics, the observed mean and standard deviation of the count of juvenile stems, and used absolute difference as the metric of comparison for both (*d* in eqn 1). We simulated 1000 particles in 9 SMC steps, with tolerance levels starting at 4 and reduced to 0.02 for both statistics (reduction of tolerance by 25% for the first two steps, 50% for the next two, and 75% for the last five).

Temporal variation in competitive environment ($CAI_{sp}$ and $CAI_{all}$) was simulated using IFN2 values for the first 90 steps of the simulation, and altering values during the final 10 time steps (corresponding to a 10-year time interval between inventories) using a linear relationship between IFN2 and IFN3 values. All algorithms (MCMC, ABC-SMC-AW and forest simulation model) were coded in C and complied in a CentOS 7.3 environment with compiler GCC 4.8.5. Statistical packages for a range of different ABC algorithms are available for use 'off-the-shelf', including several R packages (such as abc; Csilléry et al., 2012).

## Results

*ABC model implementation and fit*

Time to convergence of each ABC-SMC-AW iteration varied between species, with all but one (*P. halepensis,* Fig. 2) species' fits completing 10 iterations. Final estimate model particles' simulations had mean and standard deviation of juvenile counts within 0.02 of observations, or 0.06 for *P. halepensis* (observed means were 0.16 - 2.40 stems/5 m radius plot, standard deviations 0.63 -

4.58). We compared model predictions with data graphically and analysed posterior particle values to examine model performance. For all species, the fitted model was able to predict stem counts within the range of observations along gradients of conspecific and heterospecific crown area (Figs 2 and supporting information S4). However, model predictions did not capture all variability observed in the data for all species. Predictions are shown using mean parameter values taken from the final iteration, however for some parameters, credible intervals contained zero (Table 1), though these may be inflated as a result of the ABC approach (Csilléry et al. 2010).

*Climatic controls on probability of occurrence of juveniles*

The best-fit model probability of occurrence was the full model (eqn 3) for all but one species, and was used for all species within the simulation model (eqn 7) (details in supporting information text and Tables S9 and S10). Probability of occurrence of juveniles was strongly controlled by climate for all species, with large variation in the peak of juvenile occurrence for each species (Fig. 3). The model predicted maximum recruitment probability at higher mean annual temperatures, lower annual rainfall rates and longer droughts for Mediterranean species than temperate species (average 13.0°C vs 8.3°C, 685 mm vs 1086 mm and 0.9 months vs 0.4 months, respectively, see Fig. 3). Maximum probability of occurrence and probability predicted at the centre of each species' climatic range were higher for conifers than angiosperms (maximum 0.20 vs 0.14, average 0.10 vs 0.03), and for temperate than Mediterranean species (maximum 0.18 vs 0.14, average 0.08 vs 0.05).

*Predicted recruitment, growth and mortality rates of juveniles*

Expected recruitment rate varied strongly between species (fitted parameters Table 1), and was strongly affected by competitive environment (parameters $p_1$and $p_2$ in Table 1 and Fig. 4). In their average climatic and competitive conditions (supporting information Table S12), conifer species showed higher rates than angiosperms (19.5 vs 8.3 new 1 cm stems/ha/year) and temperate species showed higher rates than Mediterranean species (17.1 vs 12.6 stems/ha/year). Species' predicted recruitment rates in monospecific stands ($CAI_{all}$=$CAI_{sp}$) in their average climate were on average higher for temperate conifers than Mediterranean conifers, but lower for temperate angiosperm than Mediterranean angiosperms, in both low and higher density stands (Table 2). For most species, recruitment rate showed an overall hump-shaped relationship with conspecific density, with increases at low levels and declines at higher (Figs 2 and 4). Comparing from low to mid-density monospecific stands, most Mediterranean species showed a decline and most temperate species an increase in recruitment rates, but with large differences between species' rates (Table 2). Most species' recruitment rates showed a stronger negative effect of increases in conspecific than heterospecific crown area ($p_1 < p_2$ for 10 of 13 species), with on average stronger effects in higher competition (higher $p_1$ and $p_2$) for temperate than Mediterranean species.

Predicted growth and mortality rates were highly variable between species, and between groups of species (Fig. 4, supporting information Table S11). In all conditions simulated in Table 2 conifer juveniles had higher growth and mortality rates than angiosperm juveniles, and Mediterranean species had lower growth and higher mortality rates than temperate species. Growth rates of conifer species showed more rapid decline in higher competition than angiosperms (higher average $p_4$, eqn 5, Fig. 4), though there was little difference between average mortality responses, or between temperate and Mediterranean species. In species' average environments and in low monospecific stands (Table 2), mortality and recruitment rates were significantly positively correlated to each other, and to the probability of occurrence of juveniles ($p<0.05$).

Under a simple climate change scenario of +2 °C AVT, -20% AP and +20% DL, most species' probability of occurrence of recruitment and expected recruitment rates at the centre of their climate ranges showed substantial decline (Table 3). Temperate species showed a stronger decline, averaging 65%, whilst Mediterranean species had average decline of 19%. Three Mediterranean species, *P. pinea, P. halepensis* and *Q. ilex* showed increases in this changed climate (of 84%, 43% and 3% respectively).

## Discussion

### *Drivers of recruitment, growth and mortality: implications for modelling*

This study demonstrates the ability of ABC to quantify annual recruitment rates and juvenile dynamics from summarised data (Figs 2 and supporting information S4). Coarse juvenile data is widely available in national forest inventory datasets and permanent plot networks and our statistically rigorous approach could be used to both unlock understanding of processes affecting regeneration across large regions, and improve large-scale demographic model accuracy. Our approach using annual time steps accounted for time-variation in plot structure, reducing the bias in rate estimation (Kohyama et al. 2018).

We quantified the influence of climate, conspecific and heterospecific competition on juvenile processes, and found strong differences among species, even within groupings (Figs 3 and 4). Conifer species showed higher probability of occurrence and recruitment rates than angiosperms growing under similar conditions, in agreement with comparisons between Mediterranean pine and oak regeneration levels (Urbieta et al. 2011). Increasing conspecific density had a stronger effect in reducing overall recruitment rates than heterospecific competition for most species, consistent with the Janzen–Connell hypothesis and findings in plant communities worldwide (Comita et al. 2014).

We found that canopy density strongly and negatively affected juvenile recruitment and growth, and positively affected mortality rates for all species. This negative effect was on average smaller for Mediterranean species. Competition for light may be less intense in Mediterranean ecosystems due to lower leaf densities (Coomes and Grubb 2000) and facilitative effects from neighbouring trees and shrubs are known to aid seedling survival and growth, preventing desiccation by reducing water stress and protecting leaves from high levels of irradiance. Recruitment facilitation benefits reported for deciduous and Mediterranean evergreen species are stronger than those for temperate and montane *Pinus* species (Gómez-Aparicio et al. 2004, Mendoza et al. 2009).

This approach reveals recruitment patterns on scales large enough to understand and predict impacts of climate change. Although long recognised as critical for understanding forest diversity and dynamics (Kobe et al. 1995, Kobe 1996, Metz et al. 2010), studies of *rates* rather than *patterns* of recruitment have often been limited to small scales by data requirements, making predictions of change difficult. Here, we predict declines in recruitment for all species under longer drought conditions, and most under hotter temperatures, which is of particular concern given existing observed recruitment limitations (Mendoza et al. 2009) although under these conditions we predict some species may experience increases in recruitment in the cooler parts of their ranges. Warming-induced changes in recruitment rates have been observed in Spain (Peñuelas et al. 2007, Camarero and Gutiérrez 2007), and species-specific responses may be important in predicting range shifts under climate change. For example, higher rainfall has been found to increase regeneration rates of the deciduous *Q. pyrenaica* but decrease rates of the evergreen *Q. ilex* (Plieninger et al. 2010), whilst temperature is an important determinant of differential regeneration rates between species (Gómez-Aparicio et al. 2009), and seasonal drought and waterlogging may negatively affect establishment of Mediterranean oaks (Urbieta et al. 2008).

Under an scenario of increasing aridity and the frequency of climatic extremes, recruitment dynamics might be key for properly describing ecosystem responses under climate change (Matías et al. 2011, 2012). Our results show strong interspecific differences in recruitment that are likely to be critically important to robust predictions of ecosystem responses to climate change. In Spain, growth of some species may increase in a hotter future climate (Benito- Garzón et al. 2013), but our results indicate that recruitment may decrease with increasing aridity. These mismatches in demographic responses could result in ecosystem time-delayed responses and legacy effects resulting in a delayed ecosystem collapse.

*The potential of the ABC approach to exploit existing ecological data*

There are many exciting applications of ABC in ecology, for example to infer unobserved historical processes that have led to an observed state of a system (this study), or for stochastic models for which likelihoods cannot be constructed such as the neutral model of biodiversity (Jabot and Chave 2009), and these methods have been widely adopted in many areas of biological research (see Bertorelle et al. 2010). A major advantage of ABC when applied to ecological situations is that it allow the inclusion of partial knowledge of a system, whether as functional forms within a simulation model structure or as prior distributions for parameters, as demonstrated here. Whilst direct measurements of some processes may be lacking, it is unlikely that nothing is known about the direction or magnitude of *any* process within an ecological system, and the inclusion of good prior information will improve the speed of convergence of estimated parameters, and ensure ecologically reasonable output.

Despite its potential, ABC requires care in application. The multiple elements involved in calibration of the method can make it challenging to ensure that the true posterior distribution of parameters is estimated. Our choice of forest simulator (based on the PPA) was pragmatic given the structure of data available to us, but the underlying simulation model will influence ABC output and is therefore an additional source of uncertainty to consider. Model performance and validity may be influenced by the choice of summary statistics (Marin et al. 2014), but sufficiency of chosen summary statistics is difficult to establish (Marjoram et al. 2003) and optimal statistics are dataset specific (Nunes and Balding 2010). Moreover, credible intervals on posterior parameter estimates arising from ABC simulation models are likely to be inflated due to an information loss from summarised data (Csilléry et al. 2010), and ABC posterior values may not represent true probabilities (Templeton 2010). We found that, although mean trends in data were well captured by the model, predicted variability in juvenile counts was often smaller than observations (Figs 2 and supporting information S4). This is likely in part due to both the stochastic nature of recruitment, and to the fact that juvenile data was collected in a small plot size in the inventory (circular, 5 m radius), meaning microsite conditions, which may be important drivers of spatial patterns of juvenile dynamics (Vilà-Cabrera et al. 2013), are not captured within the modelling approach.

Compared to likelihood-based methods, there is less agreement on methods for ABC model comparison and goodness-of-fit (Lemaire et al. 2016), leading us to employ a pragmatic graphical approach to evaluate model performance. ABC parameterisation may be slow: the most computationally expensive element in this application was model simulation, and particle rejection rate varied strongly with species and iteration number though individual particle acceptance is independent so model simulations could be parallelised. Adoption of the ABC-SMC-AW approach (eqn 2) reduced simulations required before acceptance by an average of 27%: a figure similar to that found in Bonassi and West (2015).

## Conclusions

Our results highlight the role of juvenile stage as a driver of forest species distributions along environmental gradients. We observed strong interspecific differences, within and between functional groupings, and quantified life-history strategies and competitive effects driving species segregation. Mediterranean species had on average higher recruitment rates and maximum recruitment in warmer and drier locations, but also higher mortality of juveniles and lower growth rates than cool temperate species. The juvenile life stage is likely to be the first indicator of changes to species distributions and structural and successional dynamics in a changing climate, making best use of data on early life history crucial for defensible predictive modelling as well as designing forest restoration and adaptation strategies. Importantly, our results predict a widespread recruitment decline for most studied species, along with a few ‘winners’ in the ecosystem; all Mediterranean species. However, whether this pattern will be reflected in adult diversity may depend critically on feedbacks between species demography and interspecific interactions (e.g. Matías and Jump 2012), so models that do not capture these feedbacks may give misleading results when projecting species distributions under climate change.

The ABC method used here incorporates partial knowledge of the systems to infer critical unmeasured processes, and thus fully parameterise complex models that previously could not be fully specified. Without such an approach expensive and time-consuming repeat measurements would have been needed to understand juvenile dynamics in this system. This study demonstrates the power of the ABC approach for understanding ecological processes and highlights its potential for revealing critical unrecorded processes from existing information.

**Data Accessibility**

The second and third Spanish Forest Inventory data is available in the MAPAMA https://www.mapama.gob.es/). The climate data used is available in Gonzalo Jiménez (2010).

## References


Beaumont, M. A. 2010. Approximate Bayesian computation in evolution and ecology. - Annual Review of Ecology, Evolution, and Systematics 41: 379–406.

Beaumont, M. A. et al. 2009. Adaptive approximate Bayesian computation. - Biometrika in press.

Beckage, B. et al. 2000. A long-term study of tree seedling recruitment in southern Appalachian forests: the effects of canopy gaps and shrub understories. - Canadian Journal of Forest Research 30: 1617–1631.

Benito-Garzón, M. et al. 2013. Interspecific differences in tree growth and mortality responses to environmental drivers determine potential species distributional limits in Iberian forests. - Global Ecology and Biogeography 22: 1141–1151.

Bertorelle, G. et al. 2010. ABC as a flexible framework to estimate demography over space and time: some cons, many pros. - Mol. Ecol. 19: 2609–2625.

Bohlman, S. and Pacala, S. 2011. A forest structure model that determines crown layers and partitions growth and mortality rates for landscape-scale applications of tropical forests. - Journal of Ecology in press.

Bonassi, F. V. and West, M. 2015. Sequential Monte Carlo with Adaptive Weights for Approximate Bayesian Computation. - Bayesian Anal. 10: 171–187.

Camarero, J. and Gutiérrez, E. 2007. Response of Pinus uncinata recruitment to climate warming and changes in grazing pressure in an isolated population of the Iberian system (NE Spain). - Arctic, Antarctic, and Alpine Research 39: 210–217.

Chave, J. 1999. Study of structural, successional and spatial patterns in tropical rain forests using TROLL, a spatially explicit forest model. - Ecological Modelling 124: 233–254.

Clark, J. S. et al. 1998. Stages and spatial scales of recruitment limitation in southern Appalachian forests. - Ecological Monographs 68: 213–235.

Clarke, M. et al. 2016. Trait Evolution in Adaptive Radiations: Modeling and Measuring Interspecific Competition on Phylogenies. - The American Naturalist 189: 121–137.

Comita, L. S. et al. 2014. Testing predictions of the Janzen–Connell hypothesis: a meta-analysis of experimental evidence for distance- and density-dependent seed and seedling survival. - Journal of Ecology 102: 845–856.

Coomes, D. A. and Grubb, P. J. 2000. Impacts of root competition in forests and wetlands: a theoretical framework and review of experiments. - Ecological Monographs 70: 171–207.

Coomes, D. A. et al. 2012. A general integrative framework for modelling woody biomass production and carbon sequestration rates in forests. - Journal of Ecology 100: 42–64.

Csilléry, K. et al. 2010. Approximate Bayesian Computation (ABC) in practice. - Trends in Ecology & Evolution 25: 410–418.

Csilléry, K. et al. 2012. abc: an R package for approximate Bayesian computation (ABC). - Methods in Ecology and Evolution in press.

Ettinger, A. and HilleRisLambers, J. 2017. Competition and facilitation may lead to asymmetric range shift dynamics with climate change. - Glob Change Biol 23: 3921–3933.

Gómez-Aparicio, L. et al. 2004. Applying plant facilitation to forest restoration: A meta-analysis of the use of shrubs as nurse plants. - Ecological Applications 14: 1128–1138.

Gomez-Aparicio, L. et al. 2008. Oak seedling survival and growth along resource gradients in Mediterranean forests: implications for regeneration in current and future environmental scenarios. - Oikos 117: 1683–1699.

Gómez-Aparicio, L. et al. 2009. Are pine plantations valid tools for restoring Mediterranean forests? An assessment along abiotic and biotic gradients. - Ecol Appl 19: 2124–2141.

Gonzalo Jiménez, J. 2010. Diagnosis fitoclimática de la España peninsular: hacia un modelo de clasificación funcional de la vegetación y de los ecosistemas peninsulares españoles. - Organismo Autónomo de Parques Nacionales.

Green, P. T. et al. 2014. Nonrandom, diversifying processes are disproportionately strong in the smallest size classes of a tropical forest. - PNAS 111: 18649–18654.

Grove, A. and Rackham, O. 2001. The nature of Mediterranean Europe: an ecological history. - Yale University Press.

Hanewinkel, M. et al. 2013. Climate change may cause severe loss in the economic value of European forest land. - Nature Climate Change 3: 203–207.

Ibáñez, I. et al. 2007. Exploiting temporal variability to understand tree recruitment response to climate change. - Ecological Monographs 77: 163–177.

Jabot, F. and Chave, J. 2009. Inferring the parameters of the neutral theory of biodiversity using phylogenetic information and implications for tropical forests. - Ecology Letters 12: 239–248.

Katz, D. S. W. and Ibáñez, I. 2016. Foliar damage beyond species distributions is partly explained by distance dependent interactions with natural enemies. - Ecology 97: 2331–2341.

Kobe, R. K. 1996. Intraspecific variation in sapling mortality and growth predicts geographic variation in forest composition. - Ecological Monographs 66: 181.

Kobe, R. K. et al. 1995. Juvenile tree survivorship as a component of shade tolerance. - Ecological Applications 5: 517–532.

Kohyama, T. S. et al. 2018. Definition and estimation of vital rates from repeated censuses: Choices, comparisons and bias corrections focusing on trees. - Methods in Ecology and Evolution 9: 809–821.

Kolbe, A. E. et al. 1999. Geographic extension of an uneven-aged, multi-species matrix growth model for northern hardwood forests. - Ecological Modelling 121: 235–253.

Lemaire, L. et al. 2016. Goodness-of-fit statistics for approximate Bayesian computation. - arXiv:1601.04096 [stat] in press.

Marin, J.-M. et al. 2014. Relevant statistics for Bayesian model choice. - J. R. Stat. Soc. B 76: 833–859.

Marjoram, P. et al. 2003. Markov chain Monte Carlo without likelihoods. - Proceedings of the National Academy of Sciences 100: 15324–15328.

Matías, L. and Jump, A. S. 2012. Interactions between growth, demography and biotic interactions in determining species range limits in a warming world: The case of Pinus sylvestris. - Forest Ecology and Management 282: 10–22.

Matías, L. et al. 2011. Effects of resource availability on plant recruitment at the community level in a Mediterranean mountain ecosystem. - Perspectives in Plant Ecology, Evolution and Systematics 13: 277–285.

Matías, L. et al. 2012. Sporadic rainy events are more critical than increasing of drought intensity for woody species recruitment in a Mediterranean community. - Oecologia 169: 833–844.

McCarthy-Neumann, S. and Ibáñez, I. 2012. Tree range expansion may be enhanced by escape from negative plant-soil feedbacks. - Ecology 93: 2637–2649.

Mendoza, I. et al. 2009. Recruitment limitation of forest communities in a degraded Mediterranean landscape. - Journal of Vegetation Science 20: 367–376.

Metz, M. R. et al. 2010. Widespread density-dependent seedling mortality promotes species coexistence in a highly diverse Amazonian rain forest. - Ecology 91: 3675–3685.

MMA (Ministerio de Medio Ambiente) 1996. Segundo Inventario Forestal Nacional (1986–1996): bases de datos e información cartográfica.

MMA (Ministerio de Medio Ambiente) 2007. Tercer Inventario Forestal Nacional (1997-2007): bases de datos e información cartográfica.

Nunes, M. A. and Balding, D. J. 2010. On optimal selection of summary statistics for approximate Bayesian computation. - Statistical Applications in Genetics and Molecular Biology 9: Article34.

Pacala, S. W. et al. 1996. Forest models defined by field measurements: estimation, error analysis and dynamics. - Ecological Monographs 66: 1–43.

Peñuelas, J. et al. 2007. Migration, invasion and decline: changes in recruitment and forest structure in a warming-linked shift of European beech forest in Catalonia (NE Spain). - Ecography 30: 830–838.

Plieninger, T. et al. 2010. Large-scale patterns of Quercus ilex, Quercus suber, and Quercus pyrenaica regeneration in central-western Spain. - Ecosystems 13: 644–660.

Purves, D. W. et al. 2008. Predicting and understanding forest dynamics using a simple tractable model. - Proceedings of the National Academy of Sciences 105: 17018–17022.

Ruiz-Benito, P. et al. 2012. Large-scale assessment of regeneration and diversity in Mediterranean planted pine forests along ecological gradients. - Diversity and Distributions 18: 1092–1106.

Sisson, S. A. et al. 2007. Sequential Monte Carlo without likelihoods. - Proceedings of the National Academy of Sciences 104: 1760–1765.

Strigul, N. et al. 2008. Scaling from trees to forests: tractable macroscopic equations for forest dynamics. - Ecological Monographs 78: 523–545.

Templeton, A. R. 2010. Correcting Approximate Bayesian Computation. - Trends in Ecology & Evolution 25: 488–489.

Thuiller, W. et al. 2005. Climate change threats to plant diversity in Europe. - PNAS 102: 8245–8250.

Urbieta, I. R. et al. 2008. Soil water content and emergence time control seedling establishment in three co-occurring Mediterranean oak species. - Canadian Journal of Forest Research 38: 2382–2393.

Urbieta, I. R. et al. 2011. Mediterranean pine and oak distribution in southern Spain: Is there a mismatch between regeneration and adult distribution? - Journal of Vegetation Science 22: 18–31.

Vanderwel, M. C. et al. 2013. Climate-related variation in mortality and recruitment determine regional forest-type distributions. - Global Ecology and Biogeography 22: 1192–1203.

Vilà-Cabrera, A. et al. 2013. Patterns of Forest Decline and Regeneration Across Scots Pine Populations. - Ecosystems 16: 323–335.

Zhu, K. et al. 2015. Prevalence and strength of density-dependent tree recruitment. - Ecology 96: 2319–2327.

## Tables and figures

**Table 1** Fitted mean and 95% credible interval of recruitment parameters, from eqn 4: # new stems growing through a 1 cm DBH threshold per year= $p_0 CAI_{sp} \exp(-p_1(CAI_{all} - CAI_{sp}) - p_2 CAI_{sp})$.

| Species | $p_0$ | $p_1$ | $p_2$ |
|---|---|---|---|
| *P. sylvestris* | 75.65 (48.78, 108.79) | 3.84 (2.68, 5.04) | 26.34 (14.40, 39.21) |
| *P. uncinata* | 48.02 (25.68, 73.14) | 2.56 (0.45, 4.36) | 2.77 (-3.07, 8.99) |
| *P. pinea* | 57.69 (23.52, 97.88) | 2.06 (-1.26, 5.23) | -0.06 (-2.75, 2.96) |
| *P. halepensis* | 23.53 (3.45, 65.58) | -0.21 (-2.94, 3.11) | 7.00 (-2.50, 16.36) |
| *P. nigra* | 116.76 (55.77, 187.17) | 1.11 (0.03, 1.77) | 14.46 (6.45, 23.09) |
| *P. pinaster* | 62.48 (23.54, 108.18) | 0.73 (-1.51, 2.26) | 2.74 (-3.66, 11.82) |
| *J. thurifera* | 59.21 (34.03, 91.01) | 2.20 (-2.00, 6.00) | 5.65 (-6.74, 18.73) |
| *Q. petraea* | 32.77 (11.01, 60.46) | 2.38 (0.29, 4.37) | -0.05 (-1.94, 2.44) |
| *Q. pyrenaica* | 59.93 (28.95, 91.15) | 1.23 (0.12, 2.17) | 1.86 (-1.33, 6.29) |
| *Q. faginea* | 78.48 (24.72, 135.83) | 2.66 (-1.32, 4.79) | 10.68 (3.02, 17.02) |
| *Q. ilex* | 37.19 (8.22, 88.39) | 0.05 (-1.13, 0.95) | 13.15 (2.70, 23.33) |
| *Q. suber* | 44.91 (20.14, 77.41) | 2.25 (-0.90, 4.76) | 0.55 (-3.38, 4.94) |
| *F. sylvatica* | 51.76 (21.02, 90.42) | 1.17 (-1.01, 2.68) | 5.25 (1.45, 9.03) |

**Table 2** Predicted probability of occurrence (eqn 3) in the average environment encountered by a species, and under a scenario of 2°C increase in AVT, 20% decrease in MAP, 20% increase in DL. Expected rates of recruitment (RR, eqn 3 and eqn 4: 1 cm DBH stems/ha/year), growth (GR, eqn 5: cm/year for 1 cm DBH stem) and mortality (MR, eqn 6: annual probability of mortality of 1 cm DBH stem). Rates are calculated at the centre of each species' climatic ranges in the average competitive environment ($CAI_{all}$ and $CAI_{sp}$) and monospecific stands; a low density ($CAI_{all} = CAI_{sp} = 0.2$ ha/ha) and a higher density stand ($CAI_{all} = CAI_{sp} = 1$ ha/ha).

| *Species* | *Probability of occurrence* | *Probability of occurrence under climate change* | *Average competitive environment* | | | $CAI_{all} = CAI_{sp} = 0.2$ | | | $CAI_{all} = CAI_{sp} = 1$ | | |
|---|---|---|---|---|---|---|---|---|---|---|---|
| | | | *RR* | *GR* | *MR* | *RR* | *GR* | *MR* | *RR* | *GR* | *MR* |
| *P. sylvestris* | 1.12E-01 | 4.95E-02 | 0.43 | 0.314 | 0.016 | 8.13 | 0.413 | 0.012 | 0.00 | 0.184 | 0.030 |
| *P. uncinata* | 1.56E-01 | 8.11E-03 | 66.33 | 0.225 | 0.049 | 22.66 | 0.275 | 0.066 | 59.72 | 0.109 | 0.205 |
| *P. pinea* | 2.99E-03 | 5.51E-03 | 1.54 | 0.250 | 0.042 | 0.63 | 0.232 | 0.048 | 23.31 | 0.097 | 0.079 |
| *P. halepensis* | 8.45E-02 | 1.21E-01 | 13.64 | 0.232 | 0.022 | 7.92 | 0.251 | 0.030 | 0.23 | 0.121 | 0.097 |
| *P. nigra* | 1.35E-01 | 6.17E-02 | 28.99 | 0.214 | 0.085 | 37.64 | 0.250 | 0.103 | 0.00 | 0.101 | 0.208 |
| *P. pinaster* | 2.97E-02 | 9.73E-03 | 19.10 | 0.373 | 0.032 | 7.54 | 0.409 | 0.044 | 15.23 | 0.141 | 0.142 |
| *J. thurifera* | 2.48E-02 | 3.66E-03 | 6.24 | 0.104 | 0.028 | 4.20 | 0.083 | 0.045 | 0.66 | 0.034 | 0.253 |
| *Q. petraea* | 4.08E-03 | 2.49E-03 | 1.71 | 0.189 | 0.003 | 0.47 | 0.216 | 0.004 | 17.90 | 0.098 | 0.019 |
| *Q. pyrenaica* | 9.34E-03 | 3.72E-03 | 7.48 | 0.153 | 0.006 | 2.17 | 0.178 | 0.007 | 11.12 | 0.096 | 0.015 |
| *Q. faginea* | 1.88E-02 | 7.41E-03 | 4.54 | 0.174 | 0.008 | 3.21 | 0.179 | 0.009 | 0.00 | 0.114 | 0.016 |
| *Q. ilex* | 3.81E-02 | 3.93E-02 | 4.20 | 0.153 | 0.011 | 4.23 | 0.156 | 0.013 | 0.00 | 0.117 | 0.023 |
| *Q. suber* | 4.49E-02 | 3.74E-02 | 22.23 | 0.163 | 0.032 | 7.01 | 0.169 | 0.042 | 148.21 | 0.074 | 0.122 |
| *F. sylvatica* | 3.50E-02 | 8.24E-03 | 9.34 | 0.194 | 0.022 | 6.20 | 0.308 | 0.026 | 1.21 | 0.148 | 0.047 |

**Figure 1** Histograms of juvenile stem counts in inventory plots used for the analysis, for the 13 study species. Juveniles are here defined as trees with DBH in the range 2.5 – 7.5 cm. Plots with more than 25 observed juveniles are not shown for visual clarity, but account for no more than 1% of plots for any species.

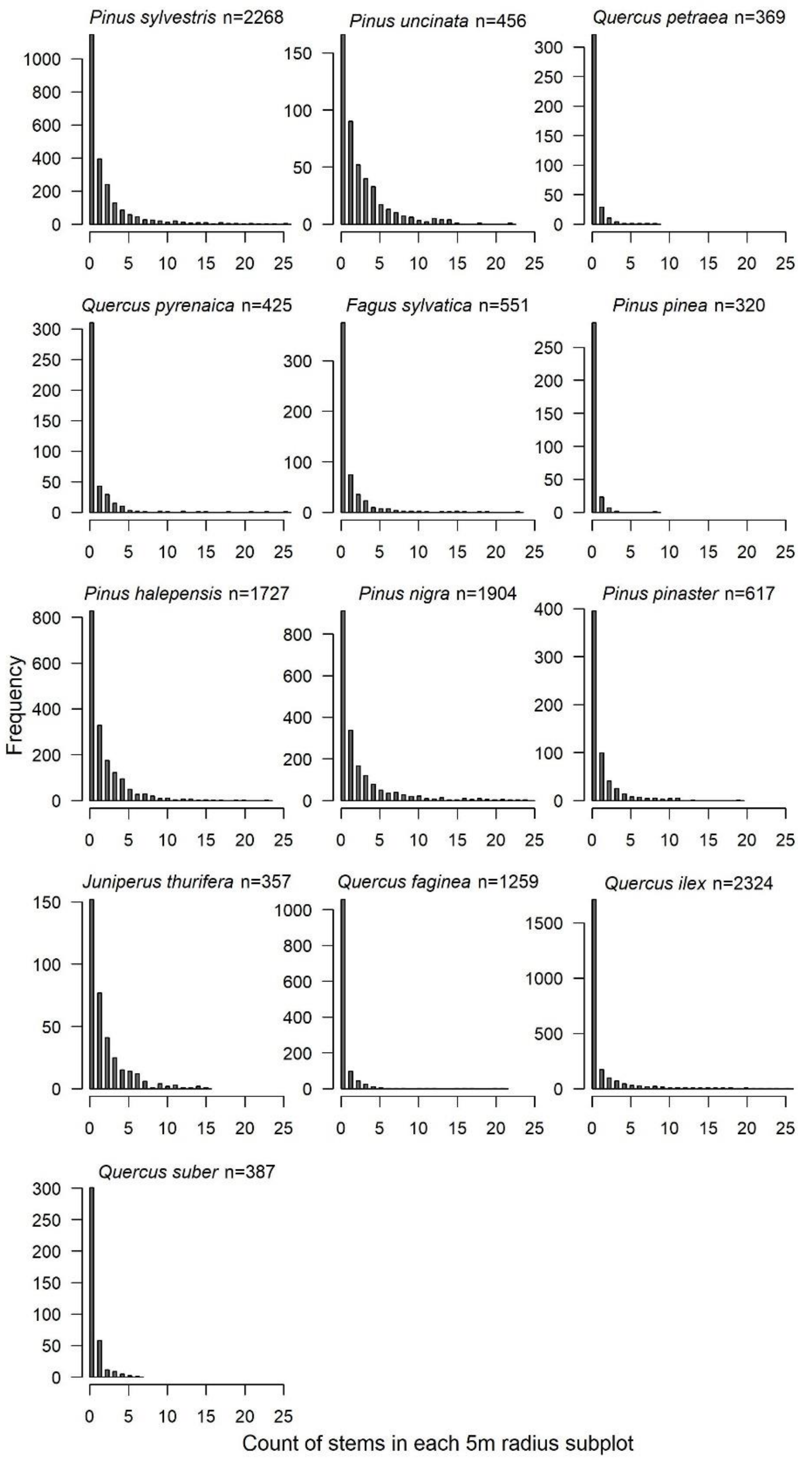

**Figure 2** Model observed (black) versus predicted (blue, offset 0.01 to the left for visual clarity) juvenile stem counts, shown along gradients of conspecific and heterospecific crown area index (*$CAI_{sp}$* and *$CAI_{all}$* - *$CAI_{sp}$*, eqn 4), for *P. halepensis* and *Q. ilex*. Model output and data plotted in bins representing 10% of plots, except where bins overlapped (for species with high numbers of monospecific plots), where bins are combined. Error bars represent 95% range (all species are shown in supporting information Fig. S4).

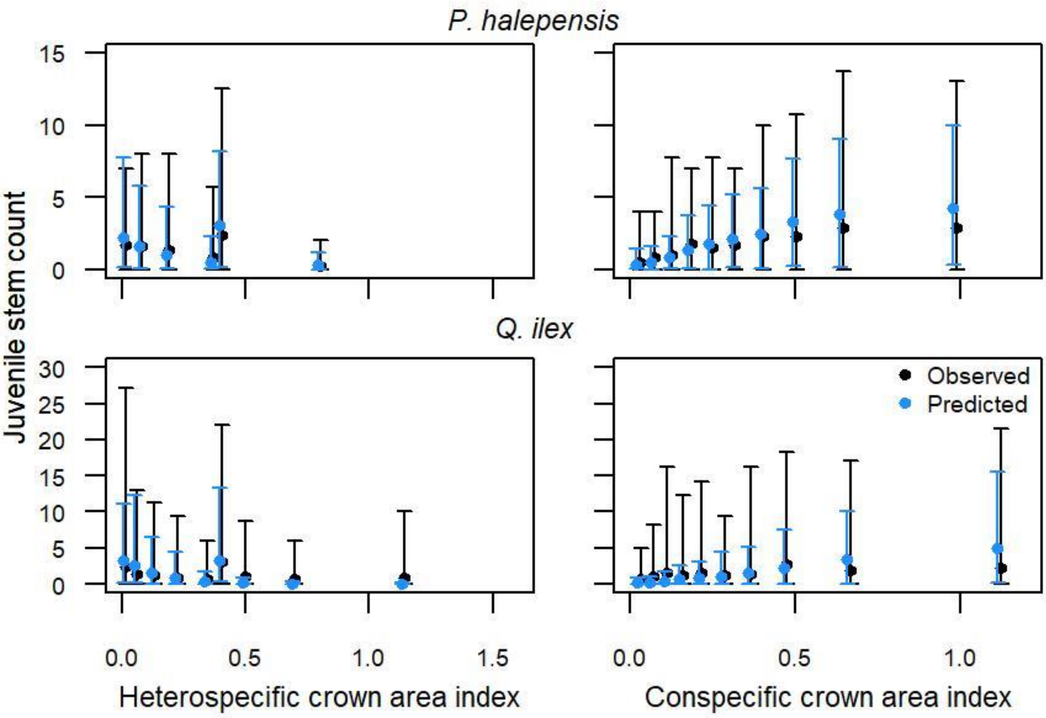

**Figure 3** Fitted probability of occurrence of juveniles across whole-data gradients of predictor variables for species of (a) temperate conifer, (b) temperate angiosperm, (c) Mediterranean conifer and (d) Mediterranean angiosperm (note differences in y-axis ranges for different species groupings). For each variable, species' probabilities of recruitment are plotted using constant values for the other two variables, which are set at the species' average values (supporting information Table S12).

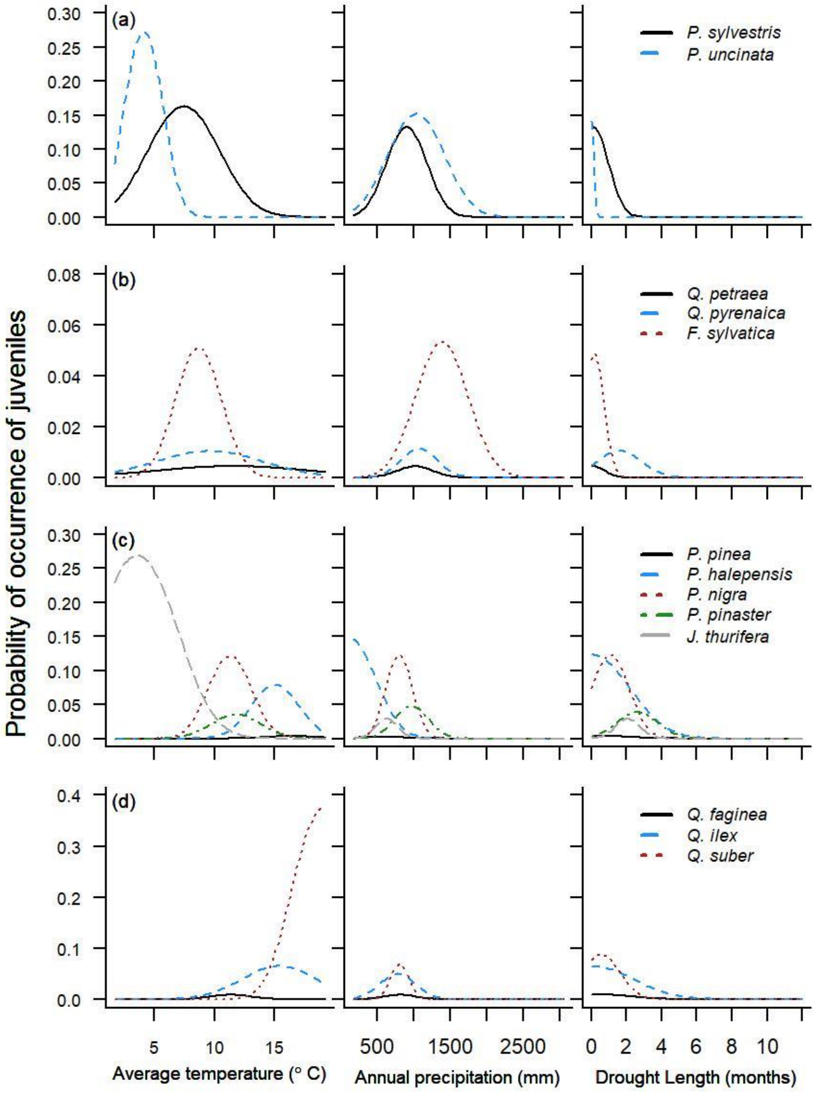

**Figure 4** Predicted rate of recruitment, growth and mortality for stems of 1 cm DBH across the observed range of total plot crown area for the species, for (column 1) conifer, and (column 2) angiosperm species. For each species, rates are calculated in the centre of the observed climatic range (calculated from the central 90% of the data see supporting information Table S12), with fixed conspecific canopy area set at the mean observed conditions.

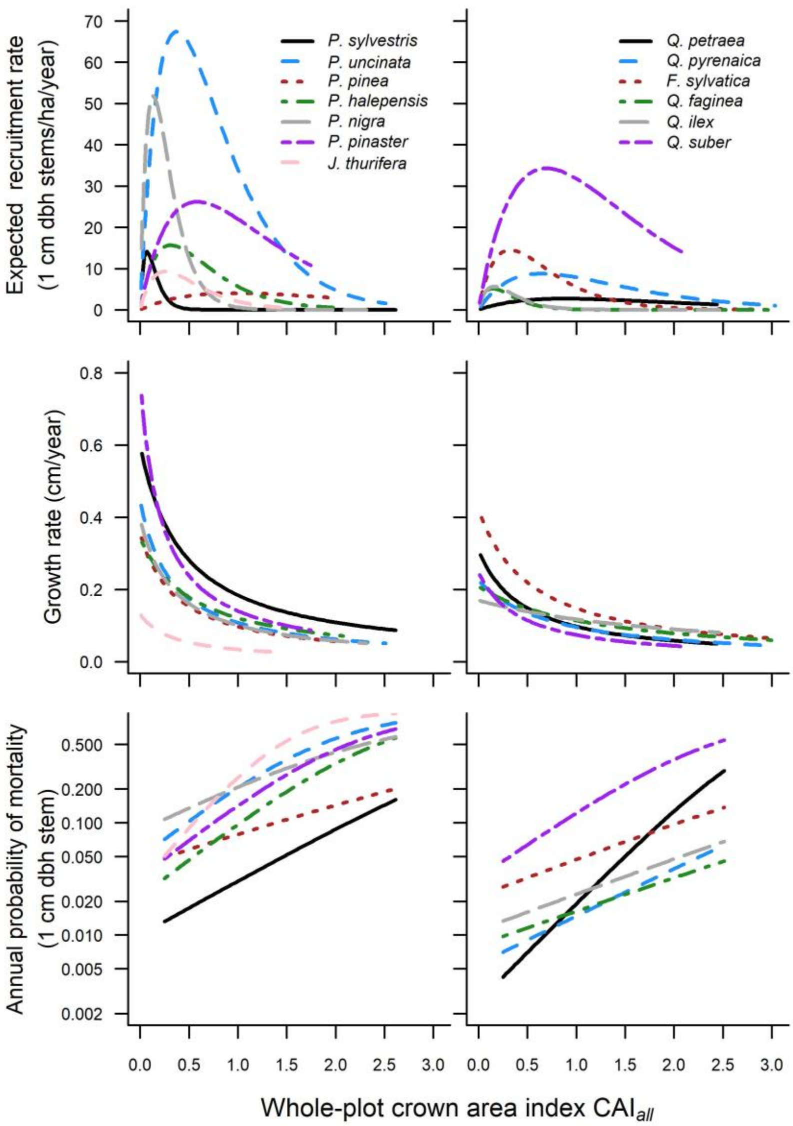

## Supplementary materials

*MCMC algorithm for fitting crown allometry and small adult growth and mortality rates*

We estimated parameters and credible intervals (CIs) of models of crown diameter, individual tree growth and annual mortality (described below) using an adaptive MCMC Metropolis algorithm (Lee 1997; Gelman, Roberts & Gilks 1999). We fitted several different functional forms for each model and compared them using the Akaike information criterion (Akaike, 1974). The MCMC algorithm compares parameter values using the log-likelihood of the data given the model. At each iteration the algorithm selects a parameter to alter and recalculates the likelihood. If the new parameter improves the likelihood then it is accepted by the algorithm. If not, it is accepted with probability of the ratio of the new and old likelihoods. In this way it returns not only a best-fit value for each parameter given the data but also estimates its distribution. The algorithm has two periods: burn-in and sampling. During the burn-in period the algorithm alters the search range ("jumping distance") of each parameter value to achieve an optimal acceptance ratio of 25% (Gelman, Roberts & Gilks 1999). After the burn-in period, the jumping distance is fixed (separately for each parameter). During sampling parameter values are recorded every 100 iterations and the resulting parameter samples are taken as samples from the posterior distribution of each parameter. The resulting samples are then used to calculate mean and 95% confidence intervals for each parameter. We used uniform priors on all parameters, setting bounds much wider than expected parameter values, so that the MCMC algorithm needed to refer to the log-likelihood only (at U[-250, 250]). We used normalised mean annual temperature and mean annual precipitation values (taken from Gonzalo Jiménez, 2008). All models were fitted using an adaptive Metropolis algorithm written in C. Convergence was checked using the Geweke diagnostic statistic (Geweke 1992), using a sampling period of 500,000 iterations of the algorithm and testing means of the initial 10% and final 50% of the chain.

*Competitive environment: crown diameter allometry and calculation of crown metric CAI*

We expected recruitment to be positively correlated with conspecific adult density (potential parent trees) and negatively with aboveground competition for light, so we generated metrics to describe these factors, choosing crown area to represent both. For each plot we defined two values to represent conspecifics adult density and aboveground competition for light; the crown cover of adults of all species of interest ($CAI_{sp}$, $m^2$/ha) and of all adults on the plot ($CAI_{all}$), using species-specific crown width allometric equations derived from data collected from the second inventory. We calculated $CAI_{all}$ and $CAI_{sp}$ for all plots in both inventories, to quantify change in canopy area over time.

We parameterised models of crown diameter (CD) as a function of stem size (DBH) and climate for each species in order to calculate the crown area of adults in each plot, both in total and of each species individually, and checked convergence using the Geweke diagnostic statistic (Geweke 1992). We used a subset of the IFN2 database in which two measurements of crown diameter were recorded for around four trees of particular silvicultural interest in each plot. The number of measurements for each species is shown in Table S1. We parameterised DBH-CD equations using adaptive MCMC for the 30 species with more than 50 trees measurements in the data (in total >200,000 measurements), which accounted for >90% of the data. We tested a set of models (see Table S2 for functional forms tested) for crown diameter as a function of stem size and climate and selected the best model as the best for the most species and data (model 10, see Table S2).

For each tree we used these functions to use to calculate the total crown area of all taller trees in each plot, $CAI_h$, and the crown area of all conspecifics, $CAI_{sp}$ in the plot. We also calculated the crown area of all trees in each plot, $CAI_{all}$. Observed and predicted crown diameters are shown for each of the 30 fitted species in Fig. S1. For species lacking allometric data we estimated the crown diameter-stem diameter relationship by either using the allometric equation of the single most closely related species or by averaging the allometric parameters of all the most closely related species if there was more than one at the closest distance (determined according to a phylogenetic tree created using the software Phylomatic, Webb & Donoghue 2005, see Table S3).

*Construction of priors for growth and mortality functions*

To construct priors for the growth and mortality functions within the ABC algorithm we fitted models to data of small trees from the Spanish Forest Inventory. We selected plots that had been measured in both the second (IFN2) and third (IFN3) inventories and fitted models to trees that had stem diameter (DBH) < 10 cm in the IFN2, excluding individuals whose mortality was human induced. We fitted models to 16 species with >100 individual stems for both growth and mortality. All models were species specific, with parameters fitted separately for each species.

Growth and mortality rates of trees are strongly size dependent, with growth increasing and mortality decreasing with size (e.g. Kunstler et al., 2009; Lines et al., 2010; Coomes et al., 2012). We compared three candidate models for growth and three candidate models for mortality using initial stem size ($DBH_1$) and competition measured as crown area of all taller trees, CAIh, in the plot (see Tables S4 and S5 for the model functional forms). For both growth and mortality, we tested a constant rate model, a size dependent model and a size and competition dependent model. We tested whether the effect of competition was important for growth using a functional form from Coomes et al. (2012) and a simple linear model for mortality. We modelled annual growth by fitting a model for the stem diameter measured in the IFN3 ($DBH_2$) as a function of the initial stem diameter measured in the IFN2 ($DBH_1$) and the growth rate using:

$$DBH_2 \sim N(DBH_1 + tGR, \omega_0^2) \qquad \text{(eqn S1)}$$

where GR is the predicted annual growth rate, t is the time interval (average 9 years) and ω0 is the standard deviation, estimated by the model.

We modelled the annual probability of mortality using a logistic function:

$$P(\text{mortality}) = 1/\big(1 + \exp(-k)\big) \qquad \text{(eqn S2)}$$

with corresponding likelihood:

$$\text{likelihood of data given model} = \begin{cases} [1 - P(\text{mortality})]^t & \text{if tree survived} \\ 1 - [1 - P(\text{mortality})]^t & \text{if tree died} \end{cases}$$

We compared a set of models with different functional for k and selected the best fit model according to AIC (see Tables S4 and S5, for model functional forms and AIC scores for growth and mortality respectively).

*Model fit results of growth and mortality model MCMC parameterisation*

We compared three models for both annual growth and annual mortality rates (Tables S4 and S5), and checked convergence using the Geweke diagnostic statistic (Geweke 1992). We calculated AIC values to compare models for each species individually. For both growth and mortality the best fit models for all species included the effects of both stem size and competition (model 2 in Tables S4 and S5), so we used these functional forms in the recruitment model. Individual species' parameter values and their corresponding 95% CIs for these two models are shown in Table S6 and S7. Predicted and observed values for $DBH_2$, fitted using model 2 in Table S4, are shown in Fig. S2. Predicted and observed values for annual mortality rate, fitted using model 2 in Table S5, are shown in Fig. S3. Predicted growth and mortality rates for each species plotted against DBH and against the range of values of $CAI_{all}$ in which it is found are shown in Fig. 3.

**Table S1** Amount of field data for each species used to estimate DBH-crown diameter allometric equations.

| Species Name | Count |
|---|---|
| *Abies alba* | 631 |
| *Abies pinsapo* | 63 |
| *Castanea sativa* | 4659 |
| *Chamaecyparis lawsoniana* | 177 |
| *Eucalyptus camaldulensis* | 1972 |
| *Eucalyptus globules* | 7127 |
| *Eucalyptus nitens* | 143 |
| *Fagus sylvatica* | 10292 |
| *Larix spp.* | 409 |
| *Picea abies* | 59 |
| *Pinus halepensis* | 30046 |
| *Pinus nigra* | 18455 |
| *Pinus pinaster* | 38086 |
| *Pinus pinea* | 8970 |
| *Pinus radiata* | 6609 |
| *Pinus sylvestris* | 28093 |
| *Pinus uncinata* | 2720 |
| *Platanus spp.* | 115 |
| *Populus alba* | 97 |
| *Populus nigra* | 1817 |
| *Pseudotsuga menziesii* | 172 |
| *Quercus canariensis* | 417 |
| *Quercus faginea* | 7845 |
| *Quercus ilex* | 36945 |
| *Quercus petraea* | 3660 |
| *Quercus pyrenaica* | 11832 |
| *Quercus robur* | 7958 |
| *Quercus rubra* | 304 |
| *Quercus suber* | 8693 |
| *Robinia pseudoacacia* | 214 |

**Table S2** Tested models of crown diameter (CD) as a function of stem size (DBH), drought length (DL), average annual temperature (AvT) and annual precipitation (PA), and the number of parameters in each model. Parameters fitted are denoted p0-p6. Average temperature and annual precipitation were normalised to aid convergence (using annual precipitation mean = 862, standard deviation = 378, average temperature mean = 12, standard deviation = 3). The number of parameters of each model, its AIC score, rank, and the number of species and percentage of the data for which it was the best model are shown. The model selected for use is shown in bold.

| Model | Description | # parameters | AIC | AIC rank | # species' best model | % data best model |
|---|---|---|---|---|---|---|
| **0** | CD ~ N($p_1$+$p_2$DBH, $p_0$) | 3 | 5593348 | 11 | 1 | 0.07 |
| **1** | CD ~ N($p_2$+$p_3$DBH, $p_0$+$p_1$DBH) | 4 | 5481178 | 7 | 5 | 16.92 |
| **2** | CD ~ N($p_1$+p2DBH+p3DL, $p_0$) | 4 | 5584746 | 8 | 0 | 0.00 |
| **3** | CD~N($p_2$+$p_3$DBH+$p_4$DL,$p_0$+$p_1$DBH) | 5 | 5472071 | 3 | 0 | 0.00 |
| **4** | CD~N($p_1$+$p_2$DBH+$p_3$AvT,$p_0$) | 4 | 5588356 | 9 | 0 | 0.00 |
| **5** | CD~N($p_2$+$p_3$DBH+$p_4$AvT,$p_0$+$p_1$DBH) | 5 | 5474664 | 5 | 2 | 1.98 |
| **6** | CD~N($p_1$+$p_2$DBH +$p_3$PA,$p_0$) | 4 | 5590359 | 10 | 0 | 0.00 |
| **7** | CD~N($p_2$+$p_3$DBH+$p_4$PA, $p_0$+$p_1$DBH) | 5 | 5478742 | 6 | 4 | 3.34 |
| **8** | CD~N($p_2$+$p_3$DBH+$p_4$DL+$p_5$AvT, $p_0$+$p_1$DBH) | 6 | 5466517 | 2 | 2 | 2.90 |
| **9** | CD~N($p_2$+$p_3$DBH+$p_4$PA+$p_5$AvT, $p_0$+$p_1$DBH) | 6 | 5472122 | 4 | 5 | 19.92 |
| **10** | **CD~N($p_2$+$p_3$DBH+$p_4$PA+$p_5$AvT+$p_6$DL, $p_0$+$p_1$DBH)** | 7 | 5464760 | 1 | 12 | 54.87 |

**Table S3** IFN species code, species genus and family, the number of plots the species was found in, and the code of the species' crown diameter allometric equations used to calculate crown area for the species (in bold if the species had its own equation), assigned using nearest phylogenetic neighbour or neighbours, if there was more than one at the closest distance. If more than one species' code is listed then the average of those species' parameters was used. For 93% of the data we were able to use crown diameter equations fitted to the individual species' crown measurements.

| IFN code | Species | Family | #Plots | IFN code(s) of species' allometric equation used to fit crown area. |
|---|---|---|---|---|
| **31** | *Abies alba* | Pinaceae | 293 | 31 |
| **32** | *Abies pinsapo* | Pinaceae | 42 | 32 |
| **7** | *Acacia spp.* | Mimosaceae | 37 | 92 |
| **76** | *Acer campestre* | Aceraceae | 902 | 41,42,43,44,45,46,47,48,51,58,61,62,64,71,72, 79,92 |
| **54** | *Alnus glutinosa* | Betulaceae | 618 | 41,42,43,44,45,46,47,48,71,72 |
| **88** | *Apollonias barbujana* | Lauraceae | 4 | 41,42,43,44,45,46,47,48,51,58,61,62,64,71,72,79, 92 |
| **68** | *Arbutus unedo* | Ericaceae | 743 | 41,42,43,44,45,46,47,48,51,58,61,62,64,71,72,92 |
| **73** | *Betula spp.* | Betulaceae | 1424 | 41,42,43,44,45,46,47,48,71,72 |
| **91** | *Buxus sempervirens* | Buxaceae | 29 | 41,42,43,44,45,46,47,48,51,58,61,62,64,71,72,92 |
| **98** | *Carpinus betulus* | Coryloideae | 5 | 41,42,43,44,45,46,47,48,71,72 |
| **72** | *Castanea sativa* | Fagaceae | 2396 | 72 |
| **17** | *Cedrus atlantica* | Pinaceae | 17 | 21,22,23,24,25,26,28,31,32,33,34,35 |
| **13** | *Celtis australis* | Ulmaceae | 18 | 41,42,43,44,45,46,47,48,71,72 |
| **67** | *Ceratonia siliqua* | Fabaceae | 218 | 92 |
| **18** | *Chamaecyparis lawsoniana* | Cupressaceae | 76 | 18 |
| **9** | *Cornus sanguinea* | Cornaceae | 1 | 41,42,43,44,45,46,47,48,51,58,61,62,64,71,72,92 |
| **74** | *Corylus avellana* | Betulaceae | 433 | 41,42,43,44,45,46,47,48,71,72 |
| **15** | *Crataegus spp.* | Rosaceae | 328 | 41,42,43,44,45,46,47,48,71,72 |
| **36** | *Cupressus sempervirens* | Cupressaceae | 71 | 18 |
| **83** | *Erica arborea* | Ericaceae | 183 | 41,42,43,44,45,46,47,48,51,58,61,62,64,71,72,92 |
| **62** | *Eucalyptus camaldulensis* | Myrtaceae | 691 | 62 |
| **61** | *Eucalyptus globulus* | Myrtaceae | 3006 | 61 |
| **64** | *Eucalyptus nitens* | Myrtaceae | 69 | 64 |
| **5** | *Euonymus europaeus* | Celastraceae | 1 | 51,58 |
| **71** | *Fagus sylvatica* | Fagaceae | 3549 | 71 |
| **3** | *Frangula alnus* | Rhamnaceae | 7 | 41,42,43,44,45,46,47,48,71,72 |
| **55** | *Fraxinus angustifolia* | Oleaceae | 761 | 41,42,43,44,45,46,47,48,51,58,61,62,64,71,72,92 |
| **1** | *Heberdenia bahamensis* | Myrsinaceae | 2 | 41,42,43,44,45,46,47,48,51,58,61,62,64,71,72,79, 92 |

| | | | | |
|---|---|---|---|---|
| **65** | *Ilex aquifolium* | Aquifoliaceae | 446 | 41,42,43,44,45,46,47,48,51,58,61,62,64,71,72,92 |
| **82** | *Ilex canariensis* | Aquifoliaceae | 114 | 41,42,43,44,45,46,47,48,51,58,61,62,64,71,72,92 |
| **75** | *Juglans regia* | Juglandaceae | 98 | 41,42,43,44,45,46,47,48,71,72 |
| **37** | *Juniperus communis* | Cupressaceae | 832 | 18 |
| **39** | *Juniperus phoenicea* | Cupressaceae | 203 | 18 |
| **38** | *Juniperus thurifera* | Cupressaceae | 1588 | 18 |
| **35** | *Larix spp.* | Pinaceae | 173 | 35 |
| **94** | *Laurus nobilis* | Lauraceae | 139 | 41,42,43,44,45,46,47,48,51,58,61,62,64,71,72,79, 92 |
| **12** | *Malus sylvestris* | Rosaceae | 32 | 41,42,43,44,45,46,47,48,71,72 |
| **81** | *Myrica faya* | Myricaceae | 202 | 41,42,43,44,45,46,47,48,71,72 |
| **87** | *Ocotea phoetens* | Lauraceae | 2 | 41,42,43,44,45,46,47,48,51,58,61,62,64,71,72,79, 92 |
| **66** | *Olea europaea* | Oleaceae | 743 | 41,42,43,44,45,46,47,48,51,58,61,62,64,71,72,92 |
| **63** | *Other/unknown eucalyptus species* | Myrtaceae | 1 | 61,62,64 |
| **89** | *Other/unknown laurel species* | Lauraceae | 6 | 41,42,43,44,45,46,47,48,51,58,61,62,64,71,72,79, 92 |
| **29** | *Other/unknown pine species* | Pinaceae | 7 | 21,22,23,24,25,26,28 |
| **59** | *Other/unknown riparian species* | Unknown (Angiosperm Average) | 6 | 41,42,43,44,45,46,47,48,51,58,61,62,64,71,72, 79,92 |
| **90** | *Other/unknown small trees* | Unknown (Angiosperm Average) | 1 | 41,42,43,44,45,46,47,48,51,58,61,62,64,71,72,79, 92 |
| **99** | *Other/unknown species* | Unknown (Angiosperm Average) | 252 | 41,42,43,44,45,46,47,48,51,58,61,62,64,71,72,79, 92 |
| **84** | *Persea indica* | Lauraceae | 43 | 41,42,43,44,45,46,47,48,51,58,61,62,64,71,72, 79,92 |
| **8** | *Phillyrea latifolia* | Oleaceae | 96 | 41,42,43,44,45,46,47,48,51,58,61,62,64,71,72,92 |
| **69** | *Phoenix spp.* | Arecaceae | 12 | 41,42,43,44,45,46,47,48,51,58,61,62,64,71,72, 79,92 |
| **86** | *Picconia excelsa* | Oleaceae | 16 | 41,42,43,44,45,46,47,48,51,58,61,62,64,71,72,92 |
| **33** | *Picea abies* | Pinaceae | 34 | 33 |
| **27** | *Pinus canariensis* | Pinaceae | 1448 | 23,24,26 |
| **24** | *Pinus halepensis* | Pinaceae | 10893 | 24 |
| **25** | *Pinus nigra* | Pinaceae | 6988 | 25 |
| **26** | *Pinus pinaster* | Pinaceae | 12372 | 26 |
| **23** | *Pinus pinea* | Pinaceae | 3288 | 23 |
| **28** | *Pinus radiata* | Pinaceae | 2368 | 28 |
| **21** | *Pinus sylvestris* | Pinaceae | 9221 | 21 |
| **22** | *Pinus uncinata* | Pinaceae | 929 | 22 |
| **93** | *Pistacia terebinthus* | Anacardiaceae | 39 | 61,62,64 |

| | | | | |
|---|---|---|---|---|
| **79** | *Platanus hispanica* | Platanaceae | 72 | 79 |
| **51** | *Populus alba* | Salicaceae | 51 | 51 |
| **58** | *Populus nigra* | Salicaceae | 658 | 58 |
| **52** | *Populus tremula* | Salicaceae | 158 | 51,58 |
| **95** | *Prunus spp.* | Rosaceae | 324 | 41,42,43,44,45,46,47,48,71,72 |
| **34** | *Pseudotsuga menziesii* | Pinaceae | 80 | 34 |
| **16** | *Pyrus spp.* | Rosaceae | 30 | 41,42,43,44,45,46,47,48,71,72 |
| **47** | *Quercus canariensis* | Fagaceae | 220 | 47 |
| **44** | *Quercus faginea* | Fagaceae | 4373 | 44 |
| **45** | *Quercus ilex* | Fagaceae | 15714 | 45 |
| **42** | *Quercus petraea* | Fagaceae | 1695 | 42 |
| **43** | *Quercus pyrenaica* | Fagaceae | 4596 | 43 |
| **41** | *Quercus robur* | Fagaceae | 3821 | 41 |
| **48** | *Quercus rubra* | Fagaceae | 154 | 48 |
| **46** | *Quercus suber* | Fagaceae | 3537 | 46 |
| **4** | *Rhamnus alaternus* | Rhamnaceae | 11 | 41,42,43,44,45,46,47,48,71,72 |
| **96** | *Rhus coriaria* | Anacardiaceae | 4 | 61,62,64 |
| **92** | *Robinia pseudoacacia* | Fabaceae | 145 | 92 |
| **57** | *Salix spp.* | Salicaceae | 702 | 51,58 |
| **97** | *Sambucus nigra* | Adoxaceae | 47 | 41,42,43,44,45,46,47,48,51,58,61,62,64,71,72, 92 |
| **78** | *Sorbus spp.* | Rosaceae | 492 | 41,42,43,44,45,46,47,48,71,72 |
| **53** | *Tamarix spp.* | Tamaricaceae | 7 | 41,42,43,44,45,46,47,48,51,58,61,62,64,71,72,92 |
| **14** | *Taxus baccata* | Taxaceae | 49 | 18 |
| **77** | *Tilia spp.* | Malvaceae | 123 | 61,62,64 |
| **56** | *Ulmus minor* | Ulmaceae | 246 | 41,42,43,44,45,46,47,48,71,72 |

**Table S4** Set of species-specific growth models tested with corresponding maximum log-likelihoods and AICs, and the number of species for which each model was the best fit (according to the AIC) out of the thirteen in the analysis. Model 2 (shown in bold) provided the best fit for the largest number of species, and was therefore chosen.

| **Model number** | **Annual growth (GR in equation S1)** | **Max log likelihood** | **# parameters** | **AIC** | **# of species' best model** |
|---|---|---|---|---|---|
| **0** | $GR=\omega_1$ | -54844.0 | 2 | 109740 | 0 |
| **1** | $GR= \omega_1 DBH$ | -54880.9 | 2 | 109813 | 0 |
| **2** | $GR=\omega_1 DBH /(1+ \omega_2 CAI_h)$ | -52217.5 | 3 | 104513 | 13 |

**Table S5** Set of species-specific mortality models tested, with corresponding maximum log-likelihoods and AICs, and the number of species for which each model was the best fit (according to the AIC) out of the thirteen in the analysis. Model 2 (shown in bold) provided the best fit for the largest number of species, and was therefore chosen.

| **Model number** | **Annual probability of mortality P(mortality)=1/(1+exp(-k)) (equation S2)** | **Max log likelihood** | **# of parameters** | **AIC** | **# of species' best model** |
|---|---|---|---|---|---|
| **0** | $k=\tau_0$ | -13147.1 | 1 | 26346.3 | 0 |
| **1** | $k=\tau_0 +\tau_1 DBH$ | -13127.5 | 2 | 26306.9 | 0 |
| **2** | $k=\tau_0 +\tau_1 DBH +\tau_2 CAI_h$ | -12467.3 | 3 | 25012.6 | 13 |

**Table S6** Parameter values and 95% confidence intervals for the chosen models for growth (equation S1) for each of the thirteen species in the analysis (model 2 in table S4). Parameters $\omega_1$ and $\omega_2$ formed prior mean values for parameters $p_3$ and $p_4$ in eqn 7 (main manuscript).

| **Species** | $\omega_0$ | $\omega_1$ | $\omega_2$ |
|---|---|---|---|
| *Fagus sylvatica* | 1.44<br>(1.39, 1.50) | 0.0470<br>(0.0428, 0.0515) | 0.000188<br>(0.000157, 0.000223) |
| *Juniperus thurifera* | 1.32<br>(1.25, 1.40) | 0.0215<br>(0.0191, 0.0241) | 0.000311<br>(0.000176, 0.000475) |
| *Pinus halepensis* | 2.10<br>(2.05, 2.15) | 0.0387<br>(0.0369, 0.0405) | 0.000180<br>(0.000154, 0.000207) |
| *Pinus nigra* | 1.92<br>(1.88, 1.97) | 0.0561<br>(0.0539, 0.0584) | 0.000307<br>(0.000279, 0.000336) |
| *Pinus pinaster* | 2.43<br>(2.43, 2.43) | 0.0934<br>(0.0934, 0.0934) | 0.000427<br>(0.000427, 0.000427) |
| *Pinus pinea* | 2.52<br>(2.36, 2.69) | 0.0670<br>(0.0600, 0.0747) | 0.000279<br>(0.000205, 0.000366) |
| *Pinus sylvestris* | 2.28<br>(2.24, 2.33) | 0.0642<br>(0.0618, 0.0667) | 0.000225<br>(0.000206, 0.000246) |
| *Pinus uncinata* | 1.86<br>(1.75, 1.98) | 0.0554<br>(0.0485, 0.0627) | 0.000348<br>(0.000261, 0.000448) |
| *Quercus faginea* | 1.10<br>(1.07, 1.13) | 0.0203<br>(0.0195, 0.0212) | 0.000084<br>(0.000069, 0.000101) |
| *Quercus ilex* | 1.50<br>(1.48, 1.52) | 0.0186<br>(0.0181, 0.0191) | 0.000046<br>(0.000038, 0.000055) |
| *Quercus petraea* | 1.98<br>(1.98, 1.98) | 0.0364<br>(0.0364, 0.0364) | 0.000201<br>(0.000201, 0.000201) |
| *Quercus pyrenaica* | 1.42<br>(1.38, 1.45) | 0.0268<br>(0.0257, 0.0280) | 0.000133<br>(0.000115, 0.000151) |
| *Quercus suber* | 1.58<br>(1.49, 1.69) | 0.0347<br>(0.0287, 0.0414) | 0.000228<br>(0.000136, 0.000339) |

**Table S7** Parameter values and 95% confidence intervals for the chosen models for mortality (equation S2) for each of the thirteen species in the analysis (model 2 in table S5). Parameters formed prior mean values for $p_5$, $p_6$ and $p_7$ in eqn 8 (main manuscript).

| **Species** | $\tau_0$ | $\tau_1$ | $\tau_2$ |
|---|---|---|---|
| *Fagus sylvatica* | -3.645<br>(-5.460,-1.573) | -0.2528<br>(-0.4939,-0.0478) | 0.000083<br>(0.000058,0.000106) |
| *Juniperus thurifera* | -2.973<br>(-5.782,-0.282) | -0.3757<br>(-0.6969,-0.0454) | 0.000245<br>(0.000099,0.000371) |
| *Pinus halepensis* | -3.645<br>(-4.555,-2.653) | -0.1316<br>(-0.2457,-0.0273) | 0.000158<br>(0.000131,0.000185) |
| *Pinus nigra* | -2.409<br>(-2.409,-2.409) | -0.3210<br>(-0.3210,-0.3210) | 0.000076<br>(0.000076,0.000076) |
| *Pinus pinaster* | -3.028<br>(-3.817,-2.152) | -0.1128<br>(-0.2138,-0.0244) | 0.000170<br>(0.000150,0.000189) |
| *Pinus pinea* | -2.243<br>(-3.786,-0.583) | -0.2087<br>(-0.3996,-0.0320) | 0.000069<br>(0.000019,0.000120) |
| *Pinus sylvestris* | -4.743<br>(-5.352,-3.945) | -0.0726<br>(-0.1628,-0.0071) | 0.000155<br>(0.000140,0.000170) |
| *Pinus uncinata* | -2.803<br>(-2.803,-2.803) | -0.1333<br>(-0.1333,-0.1333) | 0.000175<br>(0.000175,0.000175) |
| *Quercus faginea* | -4.557<br>(-5.342,-3.337) | -0.0896<br>(-0.2312,-0.0053) | 0.000086<br>(0.000053,0.000116) |
| *Quercus ilex* | -4.896<br>(-5.240,-4.357) | -0.0400<br>(-0.1027,-0.0021) | 0.000079<br>(0.000062,0.000095) |
| *Quercus petraea* | -4.812<br>(-6.669,-1.669) | -0.2020<br>(-0.5699,-0.0126) | 0.000198<br>(0.000140,0.000255) |
| *Quercus pyrenaica* | -3.933<br>(-4.577,-3.078) | -0.0820<br>(-0.1819,-0.0096) | 0.000105<br>(0.000090,0.000120) |
| *Quercus suber* | -3.124<br>(-5.033,-0.849) | -0.2281<br>(-0.4831,-0.0199) | 0.000141<br>(0.000071,0.000205) |

**Table S8** Functional forms tested for the juvenile existence model, where P(existence)=logistic(k). Here AVT = average annual temperature (°C), AP = annual precipitation (mm/year) and DL = drought length(months). (See main manuscript eqn 4).

| Model | Number of parameters | Functional form |
|---|---|---|
| 0 | 7 | $k = a_0 + a_1 a_2 AVT - a_2 AVT^2 + a_3 a_4 AP - a_4 AP^2 + a_5 a_6 DL - a_6 DL^2$ |
| 1 | 3 | $k = a_0 + a_1 a_2 AVT - a_2 AVT^2$ |
| 2 | 3 | $k = a_0 + a_1 a_2 AP - a_2 AP^2$ |
| 3 | 3 | $k = a_0 + a_1 a_2 DL - a_2 DL^2$ |
| 4 | 5 | $k = a_0 + a_1 a_2 AVT - a_2 AVT^2 + a_3 a_4 AP - a_4 AP^2$ |
| 5 | 5 | $k = a_0 + a_1 a_2 AVT - a_2 AVT^2 + a_3 a_4 DL - a_4 DL^2$ |
| 6 | 5 | $k = a_0 + a_1 a_2 AP - a_2 AP^2 + a_3 a_4 DL - a_4 DL^2$ |

**Table S9** Number of parameters and AIC for all juvenile existence model forms (table S8). Lowest values (best fit model) for each species are shown in bold. Model 0 (main manuscript eqn 4) was chosen as it was judged the best for all but one species.

| Model | 0 | 1 | 2 | 3 | 4 | 5 | 6 |
|---|---|---|---|---|---|---|---|
| Number of parameters | 7 | 3 | 3 | 3 | 5 | 5 | 5 |
| Species | | | | | | | |
| *P. sylvestris* | **10202.5** | 11689.9 | 12091.7 | 11398.9 | 10949.8 | 10813.4 | 10606.4 |
| *P. uncinata* | **1794.8** | 1869.7 | 3339.1 | 3182.2 | 1835.5 | 1833.6 | 3025.3 |
| *P. pinea* | **1156.3** | 1172.0 | 1251.6 | 1273.3 | 1158.9 | 1181.3 | 1251.6 |
| *P. halepensis* | **9656.1** | 10291.3 | 10787.4 | 11651.1 | 9817.0 | 10343.6 | 10708.5 |
| *P. nigra* | **9861.9** | 11080.1 | 11099.2 | 11112.7 | 10054.0 | 10664.0 | 10314.5 |
| *P. pinaster* | **5029.3** | 5259.2 | 5387.2 | 5205.2 | 5216.6 | 5136.8 | 5099.3 |
| *J. thurifera* | **2524.1** | 2967.5 | 3090.1 | 2849.6 | 2658.9 | 2635.3 | 2748.9 |
| *Q. petraea* | 762.6 | 836.0 | 809.4 | 772.6 | 801.5 | 776.1 | **758.8** |
| *Q. pyrenaica* | **1866.4** | 1940.8 | 1903.6 | 1927.0 | 1878.7 | 1923.0 | 1867.4 |
| *Q. faginea* | **3075.7** | 3244.0 | 3290.3 | 3324.3 | 3084.4 | 3224.3 | 3177.9 |
| *Q. ilex* | **7924.6** | 8376.4 | 8224.8 | 8560.4 | 7997.8 | 8298.8 | 8206.2 |
| *Q. suber* | **1209.9** | 1653.0 | 1677.9 | 1822.4 | 1447.7 | 1315.9 | 1643.8 |
| *F. sylvatica* | **2391.2** | 2682.2 | 2673.0 | 2550.6 | 2481.3 | 2439.9 | 2509.1 |

**Table S10.** Fitted parameter values (top) and standard deviations (bottom) for model 0 (see table S8), the chosen juvenile existence model.

| | Posterior mean parameter value | | | | | | |
|---|---|---|---|---|---|---|---|
| Species | $a_0$ | $a_1$ | $a_2$ | $a_3$ | $a_4$ | $a_5$ | $a_6$ |
| *P. sylvestris* | -11.006 | 14.941 | 0.066 | 1.809 | 7.201 | 0.196 | 0.742 |
| *P. uncinata* | -8.774 | 8.293 | 0.251 | 2.070 | 3.923 | 0.100 | 33.458 |
| *P. pinea* | -36.531 | 32.838 | 0.113 | 1.077 | 4.156 | 1.347 | 0.186 |
| *P. halepensis* | -30.870 | 30.143 | 0.133 | 0.241 | 4.350 | 0.052 | 0.120 |
| *P. nigra* | -34.680 | 22.591 | 0.170 | 1.613 | 16.366 | 2.173 | 0.474 |
| *P. pinaster* | -31.254 | 23.524 | 0.121 | 1.944 | 9.578 | 5.264 | 0.373 |
| *J. thurifera* | -14.663 | 7.377 | 0.059 | 1.259 | 22.042 | 4.102 | 1.033 |
| *Q. petraea* | -15.001 | 23.703 | 0.014 | 2.039 | 7.571 | 0.289 | 1.116 |
| *Q. pyrenaica* | -16.825 | 18.828 | 0.024 | 2.155 | 8.116 | 3.254 | 0.313 |
| *Q. faginea* | -33.643 | 22.715 | 0.180 | 1.628 | 9.944 | 0.691 | 0.151 |
| *Q. ilex* | -20.592 | 30.710 | 0.054 | 1.565 | 8.600 | 0.102 | 0.095 |
| *Q. suber* | -61.827 | 38.086 | 0.111 | 1.631 | 32.422 | 1.045 | 0.471 |
| *F. sylvatica* | -21.784 | 17.370 | 0.141 | 2.792 | 4.062 | 0.361 | 1.829 |

| | Posterior parameter standard deviation | | | | | | |
|---|---|---|---|---|---|---|---|
| Species | $a_0$ | $a_1$ | $a_2$ | $a_3$ | $a_4$ | $a_5$ | $a_6$ |
| *P. sylvestris* | 0.392 | 0.382 | 0.004 | 0.024 | 0.439 | 0.082 | 0.049 |
| *P. uncinata* | 1.956 | 0.555 | 0.022 | 0.409 | 0.981 | 0.042 | 30.239 |
| *P. pinea* | 3.301 | 0.565 | 0.010 | 0.196 | 2.914 | 0.813 | 0.039 |
| *P. halepensis* | 1.180 | 0.314 | 0.006 | 0.043 | 0.258 | 0.044 | 0.008 |
| *P. nigra* | 1.101 | 0.143 | 0.009 | 0.013 | 0.583 | 0.097 | 0.039 |
| *P. pinaster* | 0.877 | 0.332 | 0.003 | 0.364 | 0.176 | 0.178 | 0.037 |
| *J. thurifera* | 0.922 | 2.341 | 0.011 | 0.040 | 3.623 | 0.167 | 0.129 |
| *Q. petraea* | 1.847 | 6.846 | 0.010 | 0.368 | 1.517 | 0.174 | 0.313 |
| *Q. pyrenaica* | 1.219 | 4.541 | 0.007 | 0.057 | 0.875 | 0.403 | 0.080 |
| *Q. faginea* | 0.950 | 0.224 | 0.007 | 0.044 | 0.885 | 0.394 | 0.037 |
| *Q. ilex* | 0.756 | 0.495 | 0.003 | 0.021 | 0.506 | 0.109 | 0.010 |
| *Q. suber* | 1.071 | 0.550 | 0.003 | 0.027 | 1.658 | 0.370 | 0.062 |
| *F. sylvatica* | 0.988 | 0.340 | 0.011 | 0.080 | 0.536 | 0.187 | 0.444 |

**Table S11 M**ean and 95% credible interval of juvenile growth and mortality parameters (eqn 6 and 7) fitted by the ABC-SMC-AW method. Values for the recruitment parameters (eqn 5) are given in the main text.

| Species | $p_3$ | $p_4$ | $p_5$ | $p_6$ | $p_7$ |
|---|---|---|---|---|---|
| *P. sylvestris* | 0.598 (0.343, 0.838) | 2.247E-04 (1.329E-04, 3.098E-04) | -4.518 (-5.423, -3.537) | -0.077 (-0.112, -0.043) | 1.126E-04 (4.189E-05, 1.841E-04) |
| *P. uncinata* | 0.447 (0.282, 0.603) | 3.122E-04 (1.845E-04, 4.370E-04) | -2.837 (-3.536, -2.237) | -0.192 (-0.192, -0.070) | 1.615E-04 (9.611E-05, 2.259E-04) |
| *P. pinea* | 0.356 (0.162, 0.576) | 2.666E-04 (1.531E-04, 3.797E-04) | -2.901 (-3.599, -2.199) | -0.286 (-0.286, -0.162) | 6.678E-05 (3.364E-05, 9.778E-05) |
| *P. halepensis* | 0.343 (0.309, 0.379) | 1.837E-04 (1.637E-04, 2.033E-04) | -3.668 (-4.049, -3.256) | -0.149 (-0.149, -0.118) | 1.566E-04 (1.381E-04, 1.752E-04) |
| *P. nigra* | 0.398 (0.248, 0.565) | 2.942E-04 (1.628E-04, 4.358E-04) | -2.060 (-2.544, -1.587) | -0.447 (-0.447, -0.190) | 1.040E-04 (7.225E-05, 1.364E-04) |
| *P. pinaster* | 0.781 (0.446, 1.103) | 4.551E-04 (2.810E-04, 6.326E-04) | -3.280 (-4.208, -2.474) | -0.158 (-0.158, -0.064) | 1.595E-04 (9.098E-05, 2.344E-04) |
| *J. thurifera* | 0.132 (0.073, 0.213) | 2.913E-04 (1.827E-04, 4.001E-04) | -3.170 (-3.816, -2.541) | -0.529 (-0.529, -0.238) | 2.466E-04 (1.300E-04, 3.624E-04) |
| *Q. petraea* | 0.309 (0.182, 0.431) | 2.162E-04 (1.347E-04, 2.967E-04) | -5.763 (-6.978, -4.407) | -0.289 (-0.289, -0.119) | 2.019E-04 (1.130E-04, 2.852E-04) |
| *Q. pyrenaica* | 0.226 (0.141, 0.312) | 1.360E-04 (8.809E-05, 1.857E-04) | -5.115 (-6.052, -4.142) | -0.108 (-0.108, -0.054) | 9.944E-05 (5.926E-05, 1.393E-04) |
| *Q. faginea* | 0.208 (0.149, 0.265) | 8.268E-05 (5.124E-05, 1.147E-04) | -4.720 (-6.917, -2.829) | -0.125 (-0.125, -0.032) | 7.001E-05 (2.837E-05, 1.114E-04) |
| *Q. ilex* | 0.170 (0.120, 0.215) | 4.524E-05 (3.080E-05, 6.070E-05) | -4.452 (-6.055, -3.360) | -0.052 (-0.052, -0.030) | 7.485E-05 (4.729E-05, 1.032E-04) |
| *Q. suber* | 0.248 (0.141, 0.366) | 2.334E-04 (1.285E-04, 3.310E-04) | -3.165 (-3.980, -2.490) | -0.331 (-0.331, -0.146) | 1.428E-04 (8.702E-05, 1.967E-04) |
| *F. sylvatica* | 0.422 (0.269, 0.572) | 1.845E-04 (1.015E-04, 2.689E-04) | -3.504 (-4.747, -2.330) | -0.392 (-0.392, -0.157) | 7.740E-05 (4.025E-05, 1.168E-04) |

**Table S12** Species average climatic conditions, calculated at the centre of the central 90% of their climatic ranges, and the average competitive conditions in the second forest inventory (average $CAI_{sp}$ and $CAI_{all}$ in IFN2) from all plots used in the juvenile analysis.

| Species | Average annual temperature (°C) | Average annual precipitation (mm/year) | Average drought length (months) | Average $CAI_{sp}$ | Average $CAI_{all}$ |
|---|---|---|---|---|---|
| *P. sylvestris* | 9.35 | 1022.33 | 0.76 | 0.21 | 0.40 |
| *P. uncinata* | 6.40 | 1233.13 | 0.00 | 0.16 | 0.32 |
| *P. pinea* | 13.80 | 678.53 | 1.91 | 0.08 | 0.16 |
| *P. halepensis* | 13.80 | 621.20 | 2.06 | 0.14 | 0.26 |
| *P. nigra* | 10.85 | 812.00 | 1.30 | 0.15 | 0.29 |
| *P. pinaster* | 12.20 | 860.30 | 1.60 | 0.12 | 0.24 |
| *J. thurifera* | 10.56 | 699.60 | 1.96 | 0.05 | 0.09 |
| *Q. petraea* | 10.80 | 1018.40 | 0.67 | 0.14 | 0.29 |
| *Q. pyrenaica* | 11.70 | 976.60 | 1.36 | 0.18 | 0.35 |
| *Q. faginea* | 11.40 | 870.60 | 1.33 | 0.12 | 0.24 |
| *Q. ilex* | 12.75 | 803.00 | 1.93 | 0.13 | 0.25 |
| *Q. suber* | 14.65 | 784.20 | 1.92 | 0.12 | 0.23 |
| *F. sylvatica* | 9.25 | 1271.50 | 0.38 | 0.34 | 0.64 |

**Figure S1** Observed (black dots) and predicted (red line) crown diameters for each of the 30 species for which we had >50 measurements in the dataset.

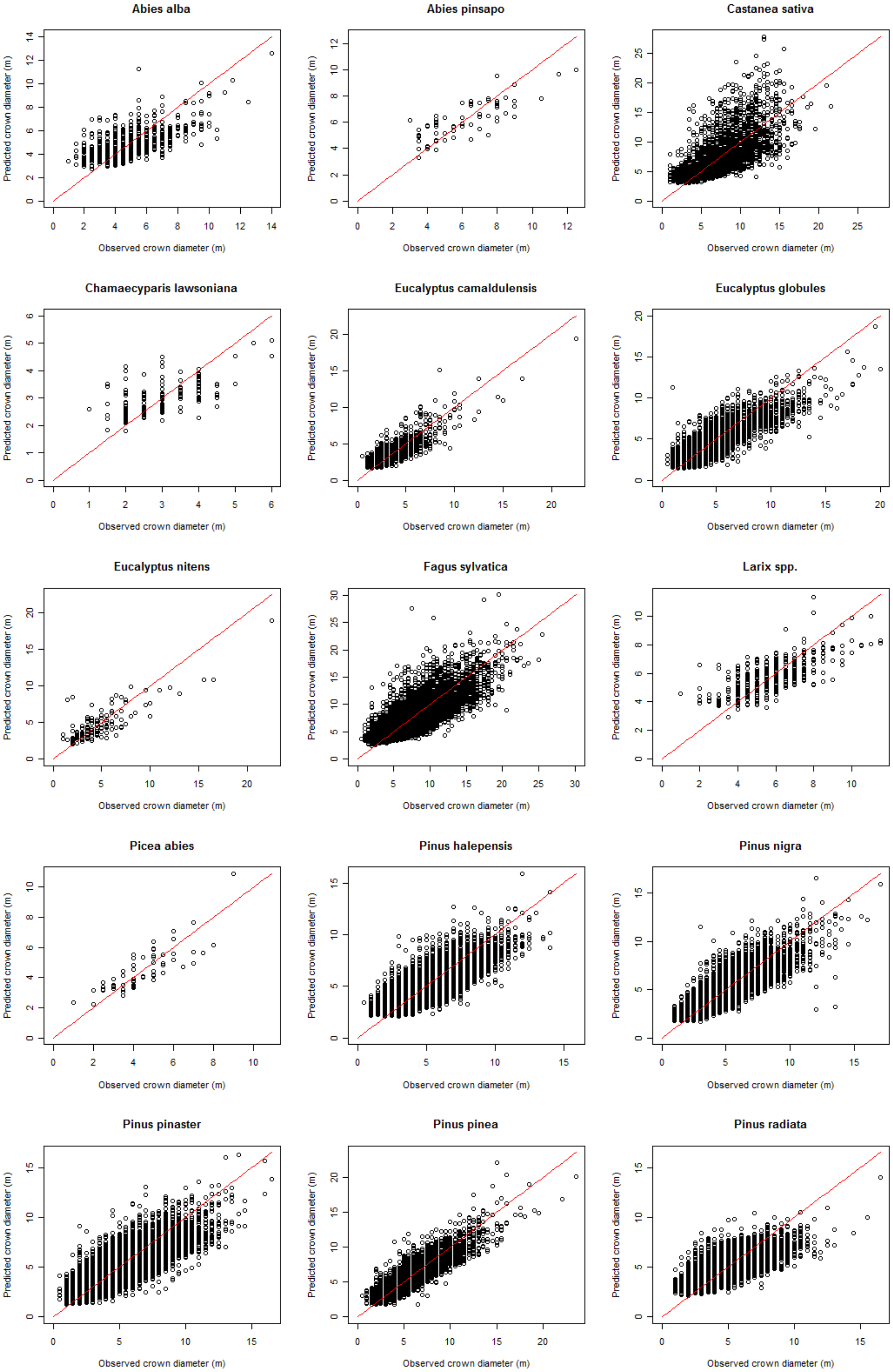

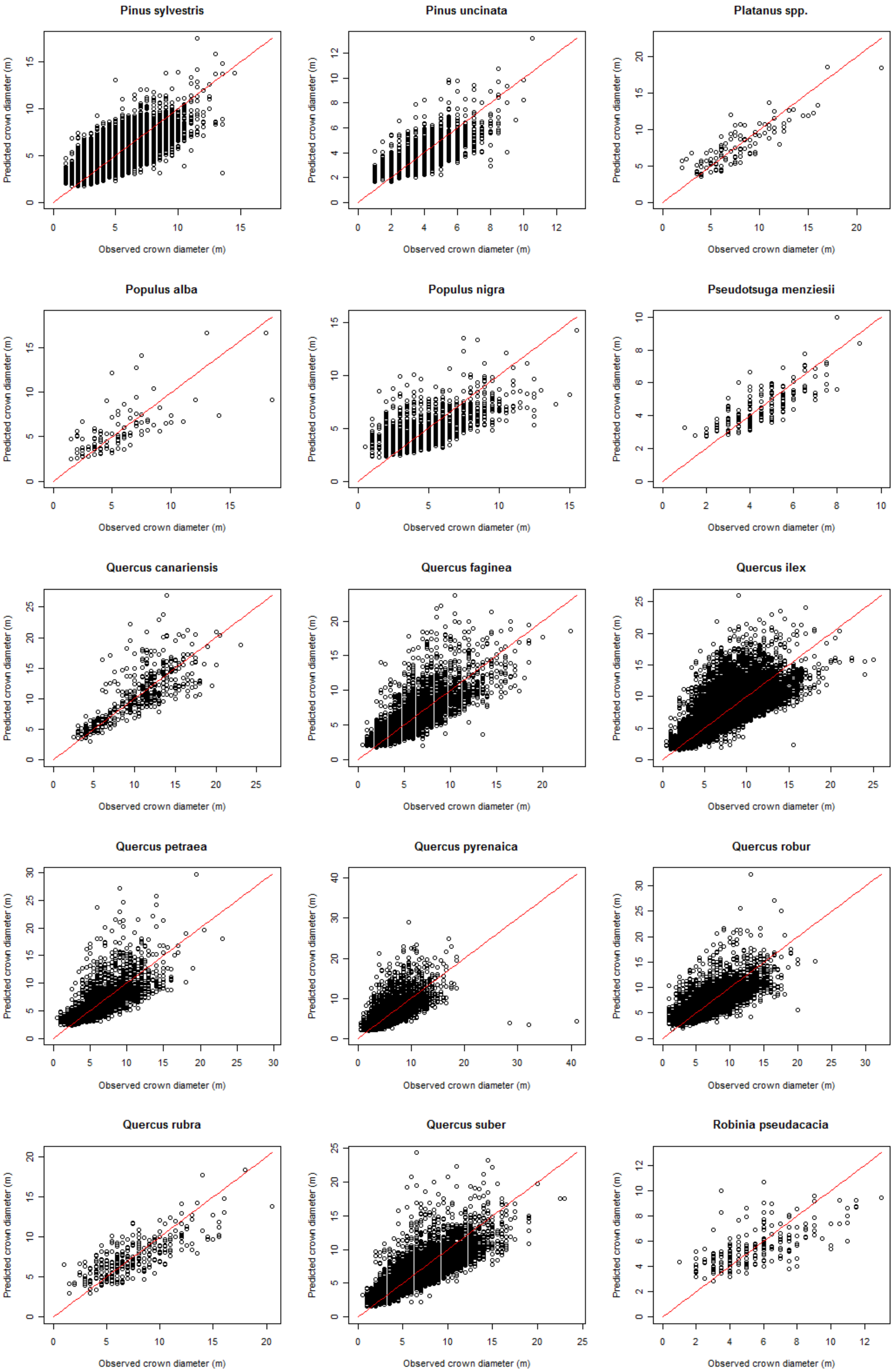
Pinus sylvestris
Pinus uncinata
Platanus spp.
Populus alba
Populus nigra
Pseudotsuga menziesii
Quercus canariensis
Quercus faginea
Quercus ilex
Quercus petraea
Quercus pyrenaica
Quercus robur
Quercus rubra
Quercus suber
Robinia pseudacacia
Predicted crown diameter (m)
Observed crown diameter (m)

**Figure S2** Predicted and observed diameters fitted using the chosen growth model (model 2 in table S4). Growth was predicted separately for each species using initial stem size ($DBH_1$) and $CAI_{all}$, and final observed diameter ($DBH_2$) is shown against predicted final diameter ($pDBH_2$). The one to one relationship is shown by the red line.

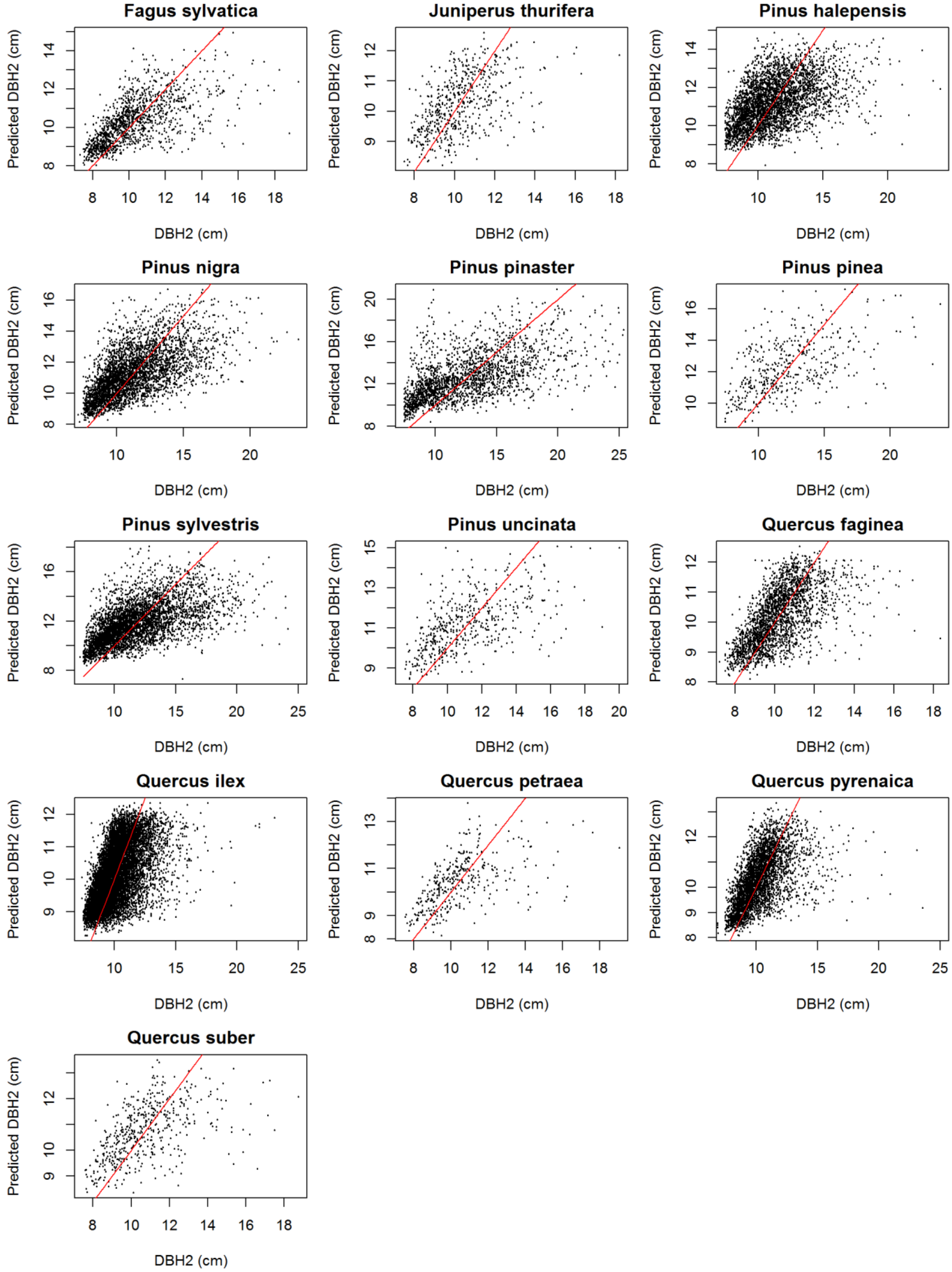

**Figure S3** Predicted and observed annual mortality fitted using the chosen mortality model (model 2 in table S5). Mortality was predicted separately for each species using $CAI_{all}$, and average rates for each species are shown with their 95% credible intervals. The one to one relationship is shown by the red line.

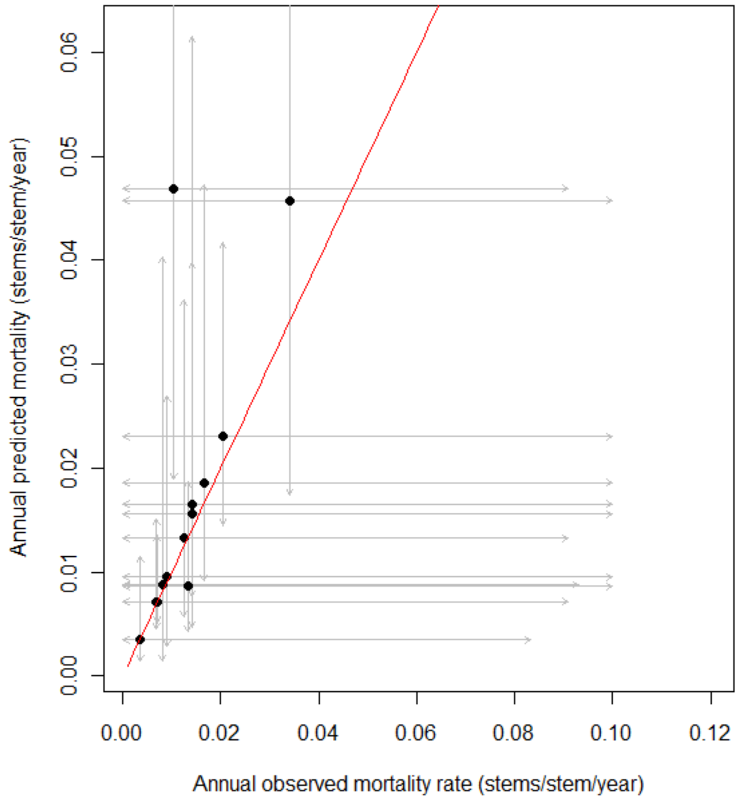

**Figure S4** Model predicted (blue) versus observed (black) juvenile stem counts, with data and predictions shown along conspecific and heterospecific crown area index ($CAI_{sp}$ and $CAI_{all}$ - $CAI_{sp}$ in eqn 5 in the main manuscript). Both model and data are binned into even sized groups representing 10% of the plots, except where bins overlapped (for species with high numbers of monospecific plots), where bins are combined, with model predictions (blue) offset by 0.01 to the left for visual clarity. Error bars represent 95% range of observations and predictions.

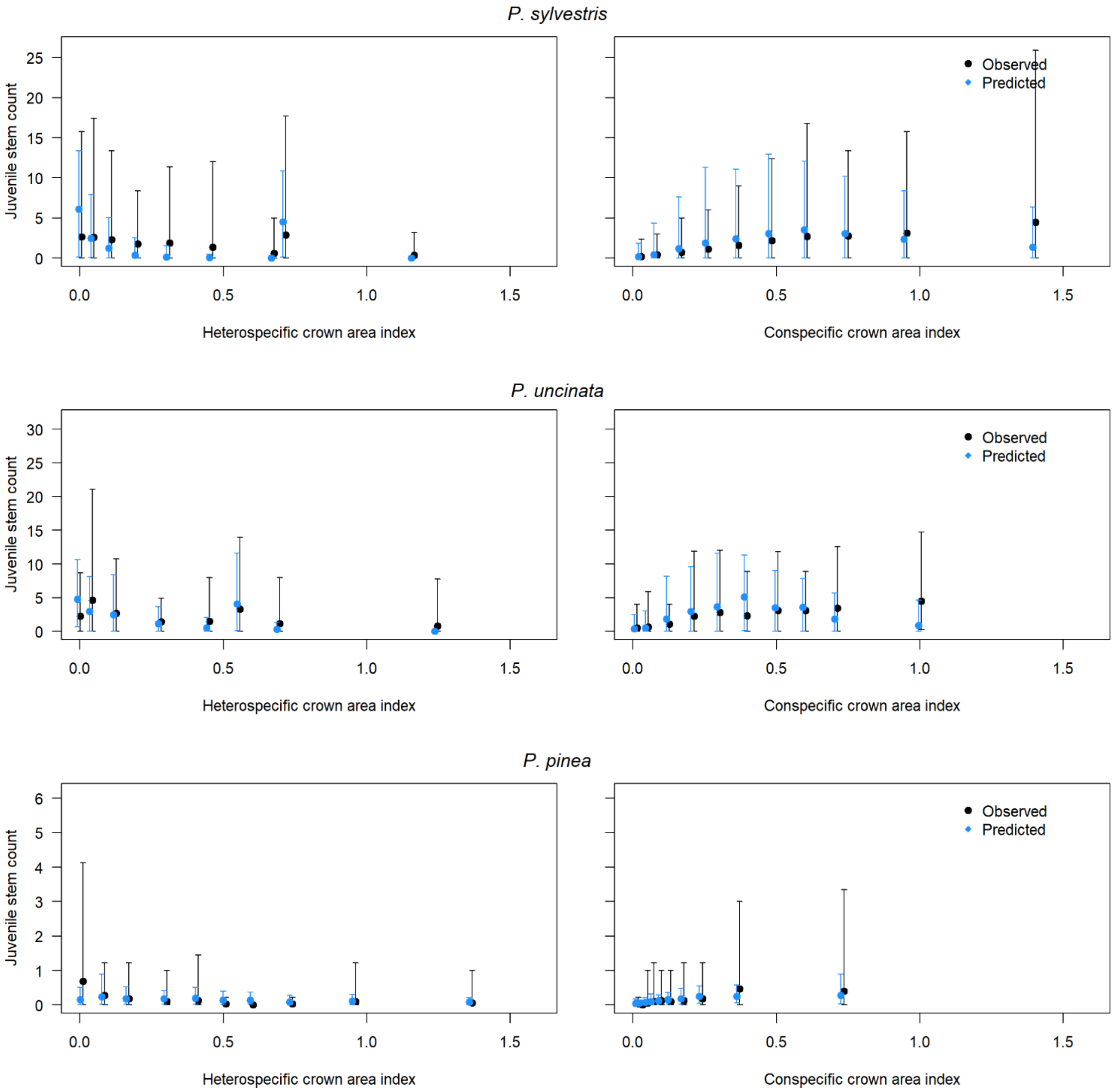

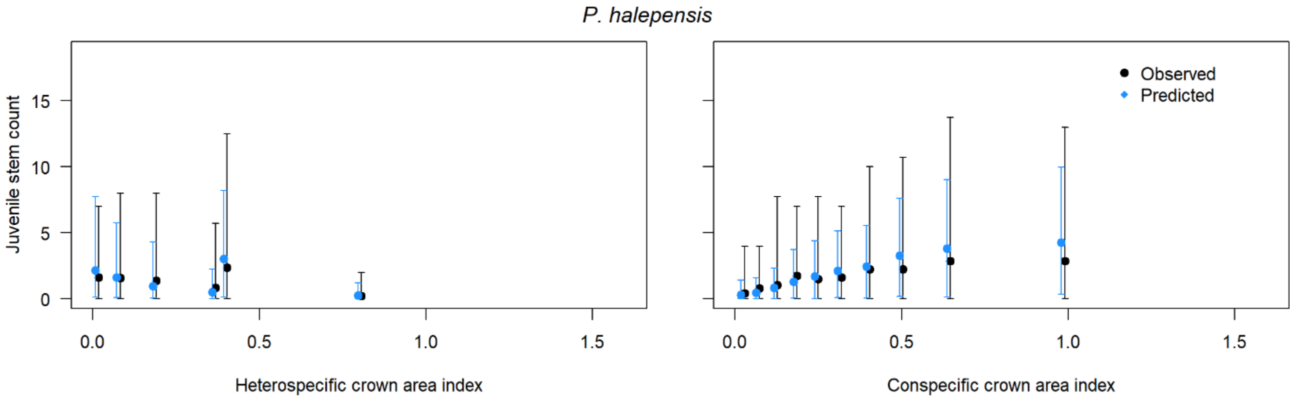

P. halepensis
Juvenile stem count
0
5
10
15
0.0
0.5
1.0
1.5
Heterospecific crown area index
Conspecific crown area index
Observed
Predicted


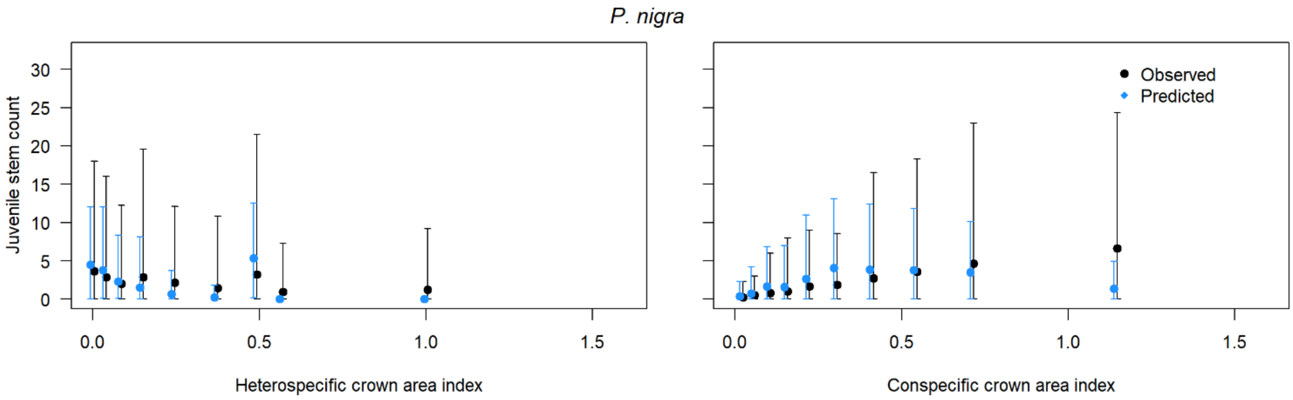

P. nigra
Juvenile stem count
0
5
10
15
20
25
30
0.0
0.5
1.0
1.5
Heterospecific crown area index
Conspecific crown area index
Observed
Predicted


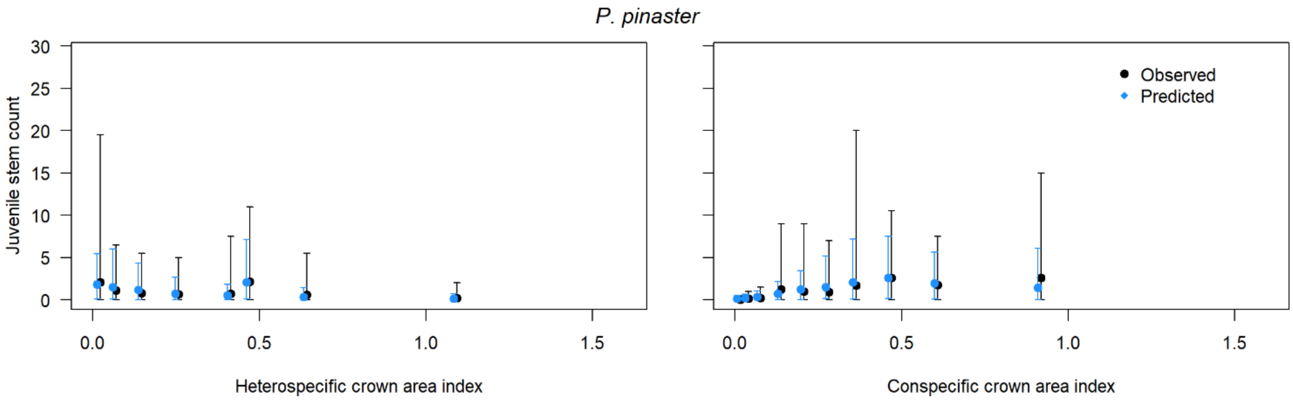

P. pinaster
Juvenile stem count
0
5
10
15
20
25
30
0.0
0.5
1.0
1.5
Heterospecific crown area index
Conspecific crown area index
Observed
Predicted


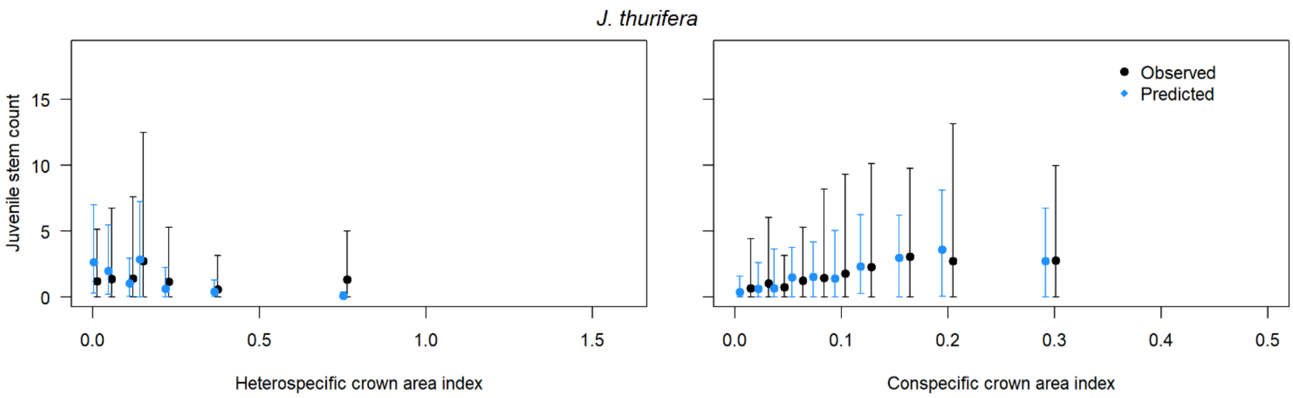

J. thurifera
Juvenile stem count
0
5
10
15
0.0
0.5
1.0
1.5
0.1
0.2
0.3
0.4
Heterospecific crown area index
Conspecific crown area index
Observed
Predicted

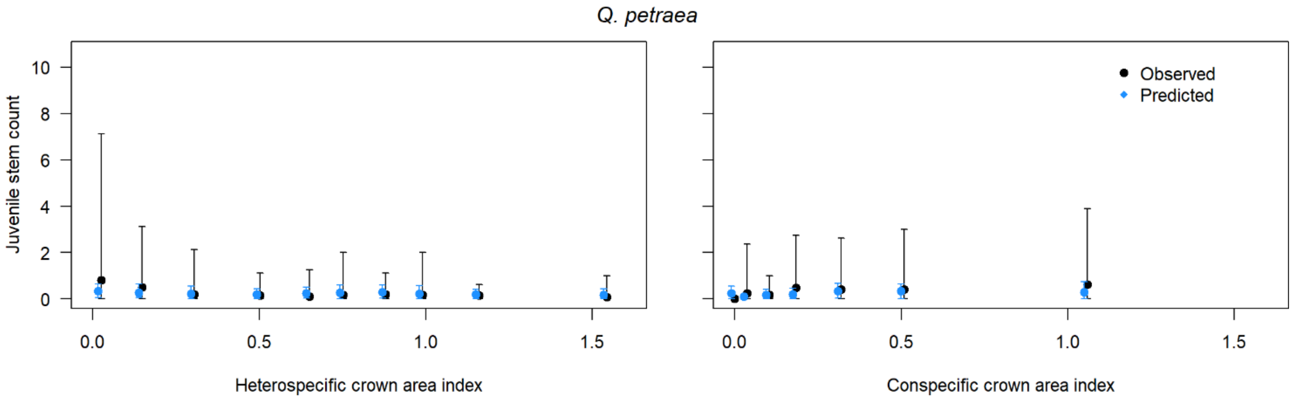
Q. petraea
Juvenile stem count
10
8
6
4
2
0
0.0
0.5
1.0
1.5
Heterospecific crown area index
Conspecific crown area index
Observed
Predicted

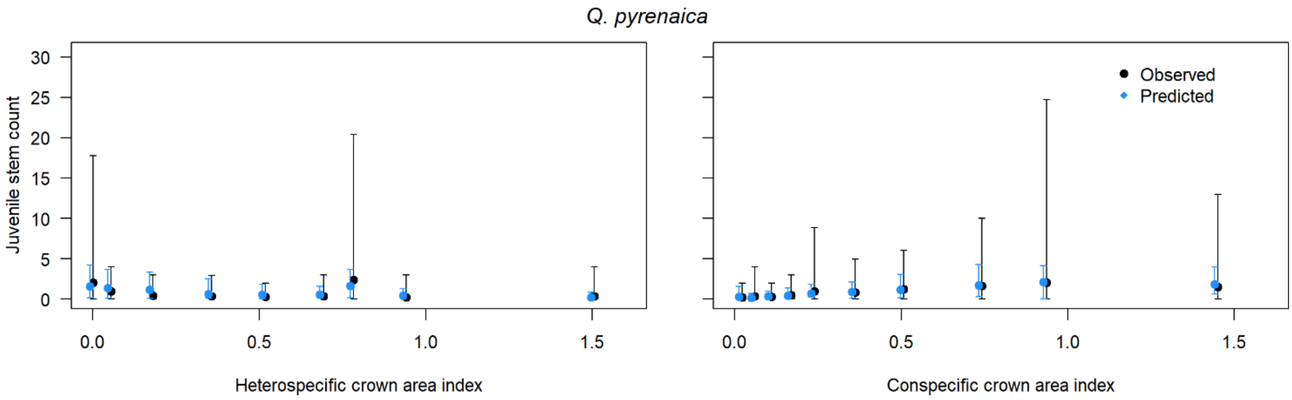
Q. pyrenaica
Juvenile stem count
30
25
20
15
10
5
0
0.0
0.5
1.0
1.5
Heterospecific crown area index
Conspecific crown area index
Observed
Predicted

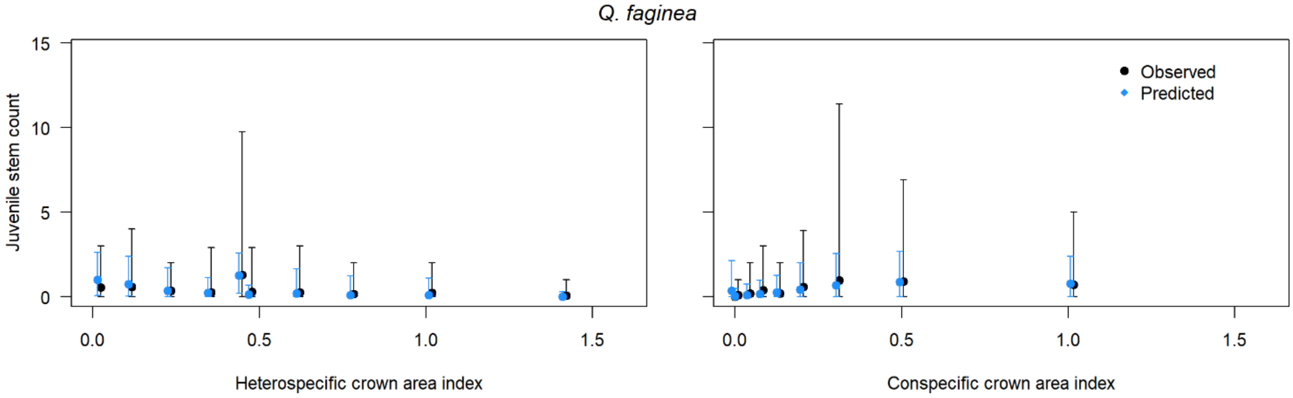
Q. faginea
Juvenile stem count
Observed
Predicted
Heterospecific crown area index
Conspecific crown area index

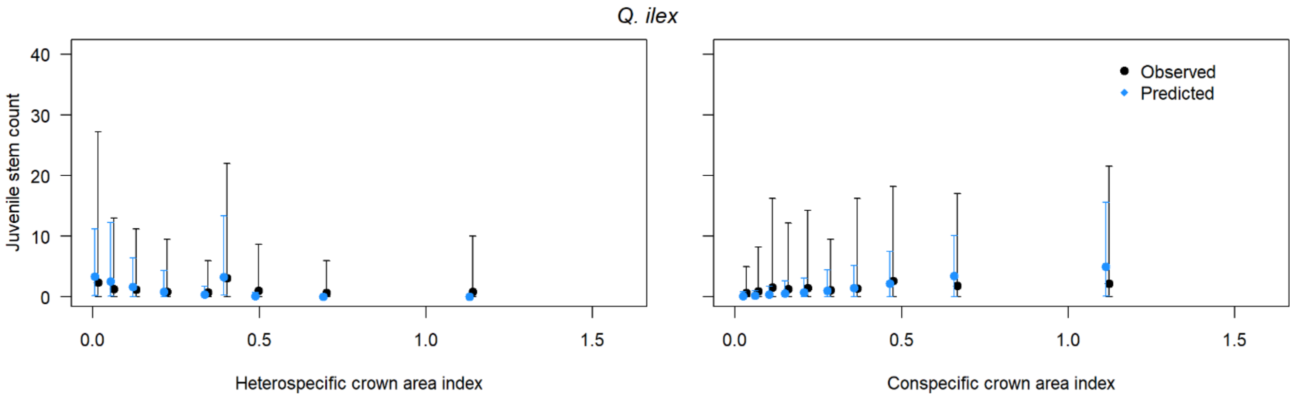
Q. ilex
Juvenile stem count
Observed
Predicted
Heterospecific crown area index
Conspecific crown area index

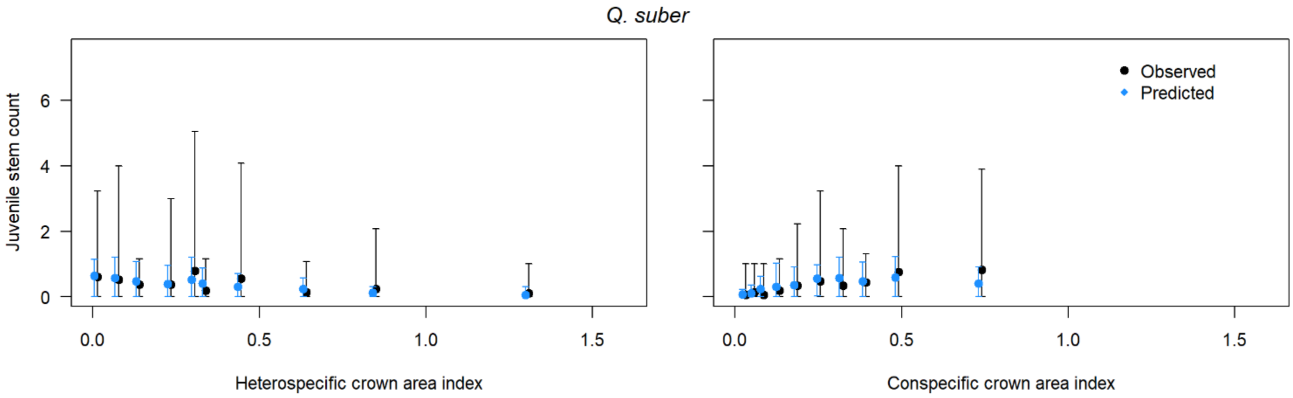
Q. suber
Juvenile stem count
Observed
Predicted
Heterospecific crown area index
Conspecific crown area index

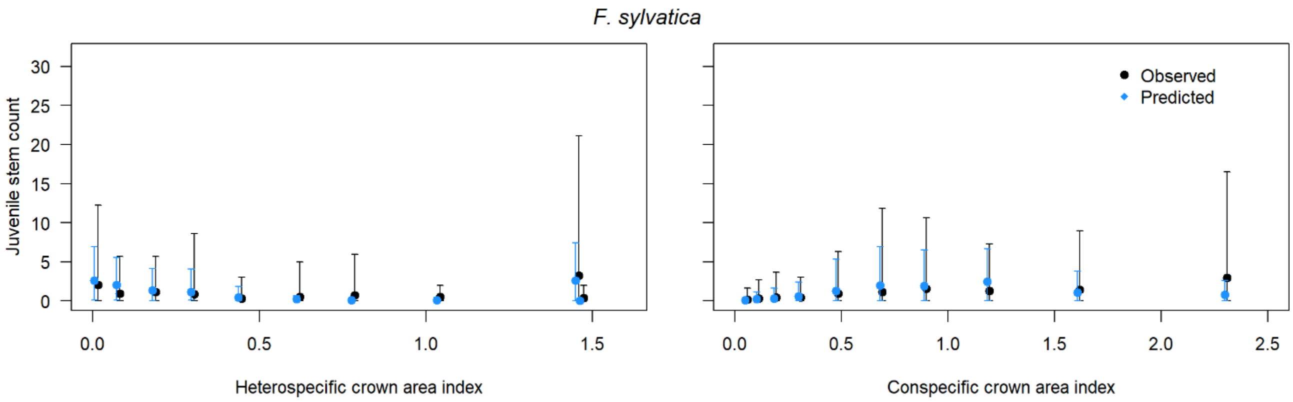
F. sylvatica
Juvenile stem count
Observed
Predicted
Heterospecific crown area index
Conspecific crown area index